Clinical outcomes in ctDNA-positive urothelial carcinoma patients treated with adjuvant immunotherapy

Authors

Thomas Powles, M.D.*+, Zoe June Assaf, Ph.D.*, Nicole Davarpanah, M.D., Romain Banchereau, Ph.D., Kobe C. Yuen, Ph.D., Petros Grivas, M.D., Maha Hussain, M.D., Stephane Oudard, M.D., Jürgen E. Gschwend, M.D., Peter Albers, M.D., Daniel Castellano, M.D., Hiroyuki Nishiyama, M.D., Siamak Daneshmand, M.D., Shruti Sharma, Ph.D., Bernhard G. Zimmermann, Ph.D., Himanshu Sethi, M.P.H, Alexey Aleshin, M.D., M.B.A, Jingbin Zhang, M.S., David S. Shames, Ph.D, Viraj Degaonkar, Pharm.D., Xiaodong Shen, Ph.D., Corey Carter, M.D., Carlos Bais, Ph.D., Joaquim Bellmunt, M.D.**, Sanjeev Mariathasan, Ph.D.**+

* Co-first authors (these authors contributed equally to this work); ** Co-last authors (these authors contributed equally to this work); + Corresponding authors.

Affiliations

Barts Cancer Institute, Queen Mary University of London ECMC, Barts Health, London, UK (T.P.); Roche/Genentech, South San Francisco, CA, USA (Z.J.A., R.B., K.C.Y., D.S.S., V.D., C.C., N.D., S.M.); University of Washington, Seattle Cancer Care Alliance and Fred Hutchinson Cancer Research Center, Seattle, WA, USA (P.G.); the Robert H. Lurie Comprehensive Cancer Center, Northwestern University, Chicago, IL, USA (M.H.); the Georges Pompidou European Hospital, University of Paris, France (S.O.); the Rechts der Isar Medical Center, Department of Urology, Technical University Munich, Germany (J.E.G.); the Heinrich-Heine University

Düsseldorf, Medical Faculty, Department of Urology, University Hospital Düsseldorf, Germany (P.A.); University Hospital 12 de Octubre, Medical Oncology Department CIBER-ONC, Madrid, Spain (D.C.); the Department of Urology, Faculty of Medicine University of Tsukuba, Ibaraki, Japan (H.N.); USC Norris Comprehensive Cancer Center, Los Angeles, CA, USA (S.D.); Natera, San Carlos, CA, USA (S.S., H.S., B.Z., A.A.); Hoffmann-La Roche Ltd, Mississauga, Ontario, Canada (J.Z.); Beth Israel Deaconess Medical Center and PSMAR-IMIM Lab, Harvard Medical School, Boston, MA, USA (J.B.).

Corresponding Authors

thomas.powles1@nhs.net and sanj@gene.com

Summary

Minimally invasive approaches to detect residual disease after surgery are urgently needed to select patients at highest risk for metastatic relapse for additional therapies. Circulating tumour DNA (ctDNA) holds promise as a biomarker for molecular residual disease (MRD) and relapse,[1-3] but its clinical value has yet to be demonstrated in a randomised clinical trial. We evaluated outcomes in post-surgical ctDNA-positive (+) patients in a randomised phase III trial of adjuvant atezolizumab versus observation. IMvigor010 enrolled 809 patients with muscle-invasive urothelial carcinoma and did not meet its primary endpoint of disease-free survival (DFS) in the intent-to-treat population. Within the study, an exploratory planned analysis of prospectively collected plasma was performed, which tested the utility of ctDNA to identify patients who may benefit from adjuvant atezolizumab treatment. ctDNA was measured at the start of therapy (cycle 1 day 1; C1D1) and at week 6 (cycle 3 day 1; C3D1), and 581 patients were evaluable for ctDNA. The prevalence of ctDNA positivity at C1D1 was 37% (n=214), and ctDNA positivity identified patients with poor prognosis (observation arm DFS HR= 6.19 (4.29, 8.91), p<0.0001). Here we show that ctDNA(+) patients had improved DFS and overall survival (OS) with atezolizumab versus observation (DFS HR= 0.56 (0.41-0.77); p=0.0003 and OS HR= 0.58 (0.4-0.86); p=0.0063). No difference in DFS or OS between arms was noted for ctDNA-negative patients. The rate of ctDNA clearance was higher with atezolizumab (18%) versus observation (4%) (p=0.0041). Transcriptomic analysis revealed that tumours from ctDNA(+) patients had higher expression of cell cycle and keratin genes. Within the ctDNA(+) patient population in the atezolizumab arm, non-relapsing patients were further enriched in prominent immune response signatures including PD-L1, IFNG, CXCL9, and high tumour mutational burden, whereas relapse was associated with angiogenesis and fibroblast-transforming growth factor-β signatures

(F-TBRS). TCGA molecular subset analysis revealed increased efficacy of atezolizumab in patients with basal-squamous tumours, consistent with underlying tumour-immune contexture. Together these findings suggest that adjuvant atezolizumab may be associated with improved outcomes compared with observation in this high-risk ctDNA(+) population. These findings, if validated in other settings, would shift approaches to post-operative cancer care.

Introduction

The use of circulating tumour DNA (ctDNA) as a biomarker of tumour burden is an emerging field in multiple solid tumour types, including urothelial, kidney, colorectal, lung, and breast cancer.[4-12] ctDNA can be differentiated from germline cell-free DNA (cfDNA) through tumour-specific somatic genomic alterations[13,14] and can be collected non-invasively from a single blood draw. ctDNA can overcome shortcomings of tissue-based biomarkers including access to tissue, use of archival samples, and tumour heterogeneity, and as a result is increasingly used to guide treatment decisions.[15-20] In the early cancer setting, ctDNA positivity has been shown to predate radiological relapse,[4,21] and is considered likely evidence of molecular residual disease (MRD).[1-3] In addition, emerging evidence indicates that clearance of ctDNA in this setting correlates with response to therapies.[22-27] Historically it has been difficult to determine which patients harbour residual disease and which are cured after surgery, despite advances in tumour staging, radiologic imaging, and tissue-based prognostic biomarkers. Therefore, many patients cured by surgery are unnecessarily exposed to adjuvant therapy toxicities, and other patients with residual disease may not receive additional treatment until disease progression is detectable by imaging (perhaps missing an opportunity to receive timely adjuvant therapy with curative intent). Detection of ctDNA shortly after surgical resection may overcome these limitations by enabling

early identification of patients harbouring MRD, who are at highest risk of relapse. Other randomised cancer trials exploring circulating biomarkers have established the prognostic value of ctDNA testing in the adjuvant setting.[28,29] It has yet to be shown in a randomised setting that ctDNA can successfully select patients for adjuvant therapy.

IMvigor010 (NCT02450331)[30] is a large, randomised adjuvant study comparing atezolizumab to observation after surgical resection for operable urothelial cancer. Atezolizumab is a monoclonal antibody that targets programmed death-ligand 1 (PD-L1) on tumour cells and tumour-infiltrating immune cells, and has been shown to have clinical efficacy in multiple tumour types including first-line UC.[18,31-35] Relapse rates after surgery for urothelial cancer are high,[36,37] and the presence of ctDNA in this setting has been shown to be a strongly negative prognostic factor as well as to predate radiological relapse with high specificity.[4] IMvigor010 did not show a significant disease-free survival (DFS) benefit in unselected patients (HR=0.89 [0.74, 1.08]; p=0.2446), nor an overall survival (OS) benefit (HR= 0.85 [0.66, 1.09]) in the interim OS analysis.[30] Therefore, this is an ideal setting to investigate the question of whether MRD(+) patients, who have a high likelihood of recurrence, can derive clinical benefit from adjuvant treatment with immune checkpoint inhibition.

Results

ctDNA was measured in the biomarker evaluable population (BEP) using established techniques (see Methods).[38,39] Briefly, whole-exome sequencing was performed on tumour and matched normal samples to identify 16 patient-specific clonal tumour mutations. These 16 mutations were used to design a bespoke multiplex PCR assay, which was run on plasma samples to detect

ctDNA with high sensitivity down to 0.01% tumour fraction. The presence of two or more of the patient-specific tumour mutations in the plasma defined ctDNA positivity, which is a threshold set by the assay vendor to maintain high specificity (>99.8[38]) and has been previously tested and validated across a number of studies.[4,9,38] Post-surgical plasma samples were collected and tested at baseline (C1D1) and 6 weeks after randomisation (C3D1). The ctDNA statistical analysis plan (SAP) was finalised before unblinding of clinical data for primary trial analysis. The primary objectives for this ctDNA study were to provide evidence that 1) within the ctDNA(+) patient population at C1D1, atezolizumab is associated with increased DFS compared with the observation arm, 2) within each arm, C1D1 ctDNA(+) status is associated with decreased DFS compared with ctDNA negative (–) status, and 3) the clearance of ctDNA in plasma by C3D1 is associated with increased DFS and clearance occurs at a higher rate in atezolizumab arm compared with observation arm. Gene expression analysis from cystectomy tissue was performed and correlated with ctDNA results. Hazard ratios (HR) for recurrence or death are reported using a multivariable Cox regression analysis adjusting for established baseline prognostic factors (nodal status, PD-L1 status, tumour stage, prior neoadjuvant chemotherapy, and number of lymph nodes resected). DFS and OS were compared between treatment groups using the log-rank test, and Kaplan-Meier methodology was applied to DFS and OS. TMB, PD-L1 and T-effector gene signatures[40] were used as established immune biomarkers.

Eight hundred and nine patients were enrolled in the IMvigor010 study (406 atezolizumab arm; 403 observation arm), with a median follow up of 21.9 months in this intention-to-treat (ITT) population. There were 581 patients (72% of the ITT population) included in the ctDNA

biomarker-evaluable patient (ctDNA BEP) population, with a median follow up of 23.0 months (**Extended Data Fig. 1a**).

Baseline characteristics of the ITT and ctDNA BEP populations were comparable and well balanced between arms (**Extended Data Tables 1 and 2**), and survival outcomes were similar between the ITT and ctDNA BEP populations for DFS (ITT stratified HR=0.89 [0.74-1.08]; p=0.2446 and BEP stratified HR= 0.88 [0.70-1.11]; p=0.2720,) as well as for OS (ITT stratified HR=0.85 [0.66-1.09] and BEP HR=0.89 [0.66-1.21]) (**Extended Data Fig. 1b-e**).

At C1D1, it was found that 37% (214/581) of patients were ctDNA(+). ctDNA positivity identified patients at higher risk of disease recurrence (observation arm DFS HR=6.19 [4.29-8.91]; p<0.0001), and shorter overall survival (observation arm OS HR= 7.92 [4.81-13.05]; p<0.0001). Analyses were repeated using a univariate approach and the results were similar (**Extended Data Table 3**). ctDNA levels were also explored as a continuous variable, and higher thresholds did not identify a group at substantially higher risk of relapse or death (**Extended Data Fig. 2**), suggesting that any presence of ctDNA is more relevant than the total burden of ctDNA in identifying high-risk patients. C1D1 collection time after surgery (median 79 days) did not associate with higher rates of ctDNA positivity or higher ctDNA levels (**Extended Data Fig. 3A-D**). ctDNA positivity at C1D1 preceded clinical relapse by radiological imaging by a median of 4.3 months (range 0.7–32.3 months) (**Extended Data Fig. 3E**). The prognostic value of ctDNA after potentially curative surgery has been described previously across a number of tumour types.[1,3,4,21]

Baseline prognostic factors and immune biomarkers (PD-L1, TMB and T- effector signatures [Teff]) were studied for association with ctDNA status, and only nodal positivity was found to correlate with ctDNA positivity (p<0.0001) (**Fig. 1e, Extended Data Table 4**). [30]

In the C1D1 ctDNA(+) population there were 116 patients in the atezolizumab arm and 98 in the observation arm, and baseline characteristics including immune biomarkers were balanced across arms (**Extended Data Table 5**). Patients in the ctDNA(+) population had improved DFS with adjuvant atezolizumab compared with patients receiving observation only (HR=0.56 [0.41-0.77]; p=0.0003, median DFS 4.4 vs 5.9 months) (**Fig. 1a**). Similarly, this ctDNA(+) patient population had improved OS with atezolizumab as compared with observation (HR= 0.58 [0.40-0.86]; p=0.0063; median OS 15.8 vs 25.8 months) (**Fig. 1b**). No difference in DFS or OS between arms was found for patients who were ctDNA(–) (DFS HR=1.07 [0.75-1.52]; p=0.7048 (median DFS not reached) and OS HR=1.22 [0.71-2.08]; p=0.4729 (median OS not reached)). Analyses were repeated using a univariate approach, and the results were similar (**Extended Data Table 6**). Thus, although the high risk of relapse for ctDNA(+) patients has been previously reported, we have shown here in this randomised phase III clinical trial setting that the poor outcomes of the ctDNA(+) patients may be improved with adjuvant atezolizumab.

In order to evaluate changes in ctDNA status in response to treatment, patients with plasma samples from both C1D1 and C3D1 were studied (485 patients, 60% of ITT). This C1D1/C3D1 BEP was analysed for similarity to the ITT population as well as for imbalances in arm and clinical factors. No imbalances were found (**Extended Data Tables 7 and 8**). At C3D1, it was found that 38.4% (186/485) of patients were ctDNA(+) and ctDNA positivity identified patients

at higher risk for disease progression and relapse (observation arm DFS HR= 8.36 [5.35-13.07]; p<0.0001). C3D1 ctDNA positivity was also a negative prognostic factor for OS (observation arm OS HR=11.80 [5.69-24.48]; p<0.0001). Results were similar when using a univariate approach (**Extended Data Table 3**).

ctDNA clearance, assessed in patients who were ctDNA(+) at C1D1 and defined in this study as achieving ctDNA(–) status by C3D1, was quantified and compared between treatment arms. It was found that clearance occurred in 18.2% (18/99) of patients in the atezolizumab arm compared with 3.8% (3/79) in the observation arm (p=0.0041) (**Fig. 2a**). Patients who cleared ctDNA within the atezolizumab arm had superior DFS and OS compared with those who did not clear (DFS HR=0.32 [0.14-0.71]; p=0.0048 and OS HR=0.17 [0.04-0.72]; p=0.0159) (**Fig. 2b-e**). Similar findings were observed when using a univariate approach **(Extended Data Table 9**). Overall, patients who were ctDNA(–) at both time points or cleared ctDNA had longer DFS than patients who were ctDNA(+) at both time points or became ctDNA(+). Reductions in ctDNA also occurred at a higher rate in the atezolizumab arm (44.4% versus 19.0% in observation, p=0.0004), which was also associated with improved outcomes (DFS HR=0.27 [0.15-0.46]; p<0.0001 and OS HR=0.32 [0.16-0.65]; p=0.0014) (**Extended Data Fig. 4**). However the DFS/OS improvement for patients who reduce ctDNA but remain ctDNA(+) was not as pronounced as is achieved by clearance of ctDNA (**Extended Data Fig. 5**).

These findings implicate the effect of atezolizumab on outcomes in ctDNA(+) patients and suggest ctDNA clearance or ctDNA reduction as a possible surrogate for treatment response. No difference in clinical outcomes between atezolizumab and observation arms were detected in

ctDNA(–) patients, implying that these lower-risk patients (63% of the ITT) may be spared adjuvant atezolizumab treatment. These findings are clinically relevant, and the selection of a high-risk group of patients who may potentially benefit from intervention using a validated blood test is attractive.

Next, we assessed the baseline transcriptional correlates of C1D1 ctDNA positivity and clinical relapse to further explore underlying mechanisms of our findings. We first applied linear modeling to identify differentially expressed genes between ctDNA(+) and ctDNA(–) patients, followed by pathway enrichment analysis using the Hallmark gene sets from MSigDB.[41] Tumours from ctDNA(+) patients were enriched in cell cycle and keratin genes (**Fig. 3a-b**), which may represent more aggressive cancer phenotypes. Within the ctDNA(+) patient population in the atezolizumab arm, non-relapsing patients were further enriched in prominent immune response signatures including PD-L1, IFNG, CXCL9, high tumour mutational burden, whereas relapse was associated with angiogenesis and fibroblast-transforming growth factor-B signatures (F-TBRS) (**Fig. 3c**). Next, we explored PD-L1 and TMB, which have previously been shown to select for response to immune checkpoint inhibitors across a spectrum of cancers in the metastatic setting.[42,43] Their role in the adjuvant setting is uncertain. In this study neither TMB nor PD-L1 could identify a subgroup that benefited from atezolizumab in the entire patient population (BEP) (**Fig. 1c-d**). However within the ctDNA(+) patient population, TMB(+) and PDL1(+) further enriches for improved clinical outcomes with atezolizumab (**Fig. 3d-f**, **Extended Data Fig. 6-8)**, which was not observed for ctDNA negative patients (**Extended Data Figs. 6, 7, and 9**). For ctDNA(+) patients, the improved outcomes with atezolizumab were even greater in triple-positive patients (ctDNA+/PDL1+/TMB+) (**Extended Data Fig. 10**). The tGE3

(CD274, IFNG, CXCL9) signature, previously shown to identify patients who respond to atezolizumab in the metastatic setting,[40] also enriched for improved outcomes on atezolizumab within the ctDNA(+) population (**Fig. 3g**). Resistance to immunotherapy in the metastastic urothelial setting is associated with high expression of the F-TBRS (pan-fibroblast TGFβ response) signature[44]. Here we show in the adjuvant setting that atezolizumab is also associated with worse outcomes in patients with high F-TBRS (**Fig. 3h**) and high angiogenesis signatures **(Fig. 3i).** These data establish the relationship between existing biomarkers of response to immunotherapy in the ctDNA(+) population. This highlights that predictive biomarkers of response must be interpreted in the context of MRD in the post-surgical setting.

TCGA studies in urothelial cancer have identified molecular subgroups with distinct clinical characteristics;[45] however it is unclear how these subtypes influence clinical outcomes in a randomised setting. Hierarchical clustering recapitulated the biological features in TCGA subgroups (**Fig. 4a**), which were distributed similarly across ctDNA(+) and ctDNA(−) patients (chi-squared p=0.21) (**Extended Data Fig. 11a**). No subgroup identified patients who had improved outcomes with atezolizumab, based on unselected patients from the biomarker evaluable population (**Extended Data Figs. 6-7**). However within the ctDNA(+) population, clinical outcomes appeared improved in the Basal-Squamous subgroup, which enriched for established biomarkers of response to immunotherapy (**Fig. 4a-f, Extended Data Fig. 11b-h,**[45]). These findings were not observed in the ctDNA(−) patients (**Fig. 4b-f, Extended Data Extended Data Figs. 6-7, and 9**). These data show specific gene signatures associated with expression and outcome in ctDNA(+) patients, and suggest TCGA analysis could be utilised in the clinical setting to better predict outcomes of patients with residual disease after surgery.

Because a subset of ctDNA(−) patients relapsed (30.6% in observation), we next analysed the baseline clinical parameters and molecular features of these patients in the observation arm (**Fig. 4g-h**). ctDNA(−) patients that do not relapse may have had successful surgery to remove the cancer. Additionally, gene expression analysis revealed the presence of pre-existing immunity in non-relapsing ctDNA(−) patients, including increased expression of interferon inducible genes (**Fig. 4g**), which may also provide some protection. In contrast, relapsing ctDNA(−) patient tumours had increases in expression of extracellular matrix, stromal, and TGFβ-inducible genes (**Fig. 4g-h)**, which may oppose any pre-existing immunity.

Because a subset of ctDNA(−) relapsed (30.6% in observation), we next analysed the baseline clinical parameters and molecular features of ctDNA(−) patients in the observation arm (**Figure 4f-h**). ctDNA(-) patients that do not relapse may have had successful surgery to remove the cancer. Additionally, gene expression analysis revealed that the presence of pre-existing immunity in non-relapsing ctDNA(-) patients, including increased expression of interferon inducible genes (**Figure 4f**), which may also provide some protection. In contrast, relapsing ctDNA(−) patient tumors had increases in expression of extracellular matrix, stromal, and TGFB-inducible genes (**Figure 4f-g)**, which may oppose any pre-existing immunity. The Luminal-Infiltrated TCGA subtype was most prominent in these patients (**Figure 4h**), which may share similar molecular and pathological characteristics of locally invasive disease. Lastly, the anatomical location of relapse differed between ctDNA(−) and ctDNA(+) patients, where ctDNA(−) relapses were associated with local relapse and ctDNA(+) with distant relapse (**Figure 4i**). These data highlight that ctDNA technologies are more sensitive at capturing metastatic

disease, whereas lower ctDNA levels are associated with specific molecular phenotypes and local relapse.

Discussion

Initiating personalised treatment based on the identification of MRD rather than treating unselected patients or waiting for relapse, would be a significant change in cancer treatment. Our analysis reveals a substantial improvement in the clinical outcomes of ctDNA(+) patients treated with adjuvant atezolizumab. These individuals are likely to have MRD after surgery. Transcriptomic analysis gave insights into the biology behind ctDNA positivity and response to atezolizumab in this population, highlighting the relevance of immune and stromal contexture. The integration of transcriptomic with ctDNA data improved our understanding of the disease and response to treatment.

While other adjuvant immunotherapy studies may be positive for DFS in unselected patients (NCT02632409), a personalised approach to select MRD(+) patients for immunotherapy may be required to demonstrate OS benefit, as well as to identify MRD(–) patients at lower risk and less likely to benefit from unnecessary treatment.

Different ctDNA technologies offer different benefits. Panel-based approaches (e.g., hybrid capture probes) are generally optimised for the most prevalent cancers (e.g., lung and colorectal), and are well-suited to genomic profiling of tumour mutations in settings where ctDNA levels are expected to be high. In contrast, personalised tumour-informed assays (such as Natera's Signatera assay used here) are well suited to any solid cancer with many tumour mutations

identifiable from tissue sequencing. Tumour-informed approaches are typically the most sensitive because they track a high number of patient-specific mutations, and therefore well-suited to post-surgical settings where clinicians need to detect residual disease with high sensitivity and specificity.[19] Newer technologies include methylation-based and fragmentomics-based approaches;[46,47] however, these methods are generally optimised for early-detection (i.e., screening), and have yet to demonstrate high clinical sensitivity in post-surgical settings.

In this study the clinical sensitivity for ctDNA at C1D1 to detect radiological relapse was 59% (observation arm), and there are a number of explanations for this finding. While we used the most sensitive assay clinically available at the time, the MRD setting is particularly challenging due to the low levels of ctDNA present in the patient after removal of the primary tumour. Non-shedding tumours may account for ctDNA(−) tumours which relapse. Other factors may also be relevant, including the timing of the ctDNA analysis (by C3D1 an additional 16 observation arm patients became ctDNA+), indolent disease resulting in delayed recurrence (mean time to relapse 4.8 months vs 10.9 months for ctDNA(+) and ctDNA(-) respectively), and anatomical location of relapse. Sequential testing ('surveillance' or 'monitoring') may increase sensitivity for ctDNA detection in the adjuvant setting[48], which is being explored in prospective trials (NCT04660344, NCT04138628). Our results also showed that the molecular profiles of the tumour may influence ctDNA positivity.

The specificity for ctDNA at C1D1 was 87% in the observation arm of our study. Several factors may affect ctDNA(+) patients who have not relapsed. Two of these patients converted to ctDNA negative by C3D1, suggesting some mechanism of spontaneous immune clearance. Other factors

include the duration of follow up, the performance of the assay, and the definition of ctDNA positivity. In this study ctDNA positivity was previously validated and predefined, which is a strength of the work. Exploration of different ctDNA methods or different definitions of ctDNA positivity may yield different results. For example, while exploring multiple cut-offs, we found that lowering the pre-defined cut-off from 2 variants to a single variant caused a ~10% reduction in specificity and identified a new cohort of patients which showed no treatment benefit with Atezolizumab. Thus, ctDNA-positivity as defined by 2 variant cut-off yielded the highest specificity while preserving sensitivity.

We acknowledge several limitations of our study. ctDNA status was a prospective but exploratory endpoint and therefore further studies in urothelial cancer and other tumour types are required to validate and expand its clinical utility. Also, plasma testing was only available for two time points in the study (C1D1 and C3D1), and it is unknown if these are the optimal time points. This method of ctDNA analysis required whole exome sequencing (WES) and takes approximately 2-3 weeks. This is clinically applicable in the adjuvant setting where patients require a significant period of time to recover from surgery before starting adjuvant therapy.

These novel and provocative findings demonstrate ctDNA as a marker for MRD and response to atezolizumab. The ctDNA findings are closely linked to the biology of the tumours, giving insight into the generation of ctDNA and mechanisms of response to immune therapy. These data change our understanding of post-surgical cancer care. If validated in this setting, as well as across tumour types, they will change clinical practice.

Acknowledgments

The study was sponsored by F. Hoffmann-La Roche Ltd./Genentech, Inc., a member of the Roche Group. We thank the patients who participated in the trial and the clinical site investigators, and the Barts Health Experimental Cancer Medicine Center (CRUK). Medical writing assistance for this manuscript was provided by Harbeen Grewal and Zachary Augur of Anshin Biosolutions, Meenakshi Malhotra, PhD, of Natera, and Ashley J. Pratt, PhD, of Health Interactions, Inc., and funded by F. Hoffmann-La Roche Ltd. We would like to thank Angela Yiu and Mate Ravasz from Fios Genomics for additional help with transcriptomic analysis. We would also like to thank Susan Flynn, Katarina Zvonar, and Deepali Rishipathak of the Genentech Biomarker Operations Team for providing support in the generation and analysis of the data and Edward E. Kadel, III from the Genentech Biomarker Development team for data integration.

Author contributions

T.P., N.D., R.B., P.G., M.H., S.O., J.E.G., P.A., D.C., H.N., S.D., S.S., B.G.Z., H.S., J.Z., D.S.S., V.D., X.S., C.C., C.B., J.B., and S.M. conceived and designed the study. Z.J.A., N.D., B.G.Z., A.A., and S.M. developed the methodology. N.D., V.D., and S.M. conducted the literature search. T.P., N.D., H.S., A.A., J.B., and S.M. collected the data. T.P., Z.J.A., N.D., R.B., K.C.Y., H.S., A.A., D.S.S., V.D., C.C., C.B., J.B., and S.M. analysed and interpreted the data. Z.J.A., S.S., A.A., and J.Z. contributed to the development of the statistical analysis plan and/or conducted the statistical analysis. All authors drafted and revised the manuscript. All authors critically revised the manuscript for intellectual content. Z.J.A., N.D., and S.M. wrote the original draft. H.S. provided administrative, technical, or material support. T.P., P.G., M.H.,

J.E.G., D.C., and J.B. selected candidates and recruited and treated patients. T.P., M.H., J.E.G., D.C., and J.B. were part of the steering committee. All authors approved the final version of the submitted report and agree to be accountable for all aspects. All authors verify that this study was done per protocol and vouch for data accuracy and completeness.

Competing interests

T.P. received honoraria from advisory/consultancy roles with AstraZeneca, BMS, Exelixis, Incyte, Ipsen, Merck, MSD, Novartis, Pfizer, Seattle Genetics, Merck Serono (EMD Serono), Astellas, Johnson & Johnson, Eisai, and Roche; institutional research funding support from AstraZeneca, Roche, BMS, Exelixis, Ipsen, Merck, MSD, Novartis, Pfizer, Seattle Genetics, Merck Serono (EMD Serono), Astellas, and Johnson & Johnson; and travel, accommodation, and expenses support from Roche, Pfizer, MSD, AstraZeneca, and Ipsen. **Z.J.A.** discloses employment with Genentech, previous employment with Natera, and stock and other ownership interests with Roche. **N.D.** discloses employment with Genentech and stock and other ownership interests with Roche. **K.Y.C.** discloses employment with Genentech and stock ownership interests with Roche. **P.G.** received consulting fees from AstraZeneca, Bayer, Bristol Myers Squibb, Clovis Oncology, Driver, Dyania Health, EMD Serono, Exelixis, Foundation Medicine, GlaxoSmithKline, Genentech, Genzyme, Heron Therapeutics, Immunomedics, Janssen, Merck, Mirati Therapeutics, Pfizer, Roche, Seattle Genetics and QED Therapeutics; and institutional research funding support from AstraZeneca, Bavarian Nordic, Bayer, Bristol Myers Squibb, Clovis Oncology, Debiopharm, Genentech, GlaxoSmithKline, Immunomedics, Kure It Cancer Research, Merck, Mirati Therapeutics, OncogeneX, Pfizer and QED Therapeutics. **M.H.** received honoraria or advisory fees from Pfizer, AstraZeneca, Bayer, Genentech, PER, Projects

in Knowledge, Astellas Pharma, Sanofi/Genzyme, Research to Practice, BMS, and Daiichi Sankyo, research funding support from AstraZeneca, Genentech, Pfizer, and Bayer, and travel, accommodation, or expenses support from Pfizer, Bayer, Astellas Pharma, and Genentech/Roche. MH also has two pending patents and one licensed patent with Imbio to disclose. **S.O.** received advisory/consulting fees and honorarium from Astellas, Bayer, Bristol Myers Squibb, Eisai, Janssen, Merck Sharp & Dohme, Novartis, Pfizer, and Sanofi, research funding support from Ipsen and Sanofi, and travel, accommodation, or expenses support from Bayer, Bristol Myers Squibb, Eisai, Merck Sharp & Dohme, Novartis, and Pfizer. **J.E.G.** received consulting fees or honoraria from Amgen, AstraZeneca, Bayer, Janssen-Cilag, Merck, MSD, Pfizer, Roche, and Bristol Myers Squibb. **P.A.** received advisory/consulting fees and honoraria from MSD Oncology, Sanofi, and Roche/Genentech. **D.C.** received consulting fees from Astellas Pharma, AstraZeneca, Bayer, Boehringer Ingelheim, Bristol Myers Squibb, Ipsen, Janssen Oncology, Lilly, MSD Oncology, Novartis, Pfizer, Pierre Fabre, Roche/Genentech, and Sanofi, research funding support from Janssen Oncology, and travel, accommodation, or expenses support from AstraZeneca Spain, Bristol Myers Squibb, Pfizer, and Roche. **H.N.** received research funding support from Ono and Chugai, consulting fees from Bayer, Chugai, Bristol Myers Squibb, Astellas, MSD, Janssen, and AstraZeneca, and participated in Speakers' Bureaus for Chugai, MSD, Astellas, and AstraZeneca. **S.D.** received honoraria from Ferring, Olympus, Pacific Edge, Photocure, QED, MDxHealth, and Spectrum Pharmaceuticals, advisory fees from Ferring, Photocure, QED, and Taris, and research funding, travel, accommodation, or expenses support from Photocure. **S.S.** discloses employment with Natera. **B.G.Z.** discloses employment with and owns stock or other ownership interests in Natera. **H.S.** discloses employment with Natera. **A.A.** discloses employment with Natera. **J.Z.** discloses employment

with Hoffman-La Roche. **R.B.** discloses employment with and owns stock or other ownership interests in Genentech. **D.S.S.** discloses employment with Genentech and owns stock or other ownership interests in Roche. **V.D.** discloses employment with Genentech and owns stock or other ownership interests in Roche. **X.S.** discloses employment with and owns stock or other ownership interests in Genentech. **C.C.** discloses employment with Genentech. **C.B.** discloses employment with Genentech. **J.B.** received advisory/consulting fees from Astellas Pharma, AstraZeneca/MedImmune, Bristol-Myers Squibb, Genentech, Merck, Novartis, Pfizer, and Pierre Fabre; honoraria from UpToDate; research funding support from Millennium, Sanofi, and Pfizer/EMD Serono; owns stock or other ownership interests in Rainer; and travel, accommodation, or expenses support from Pfizer, MSD Oncology, and Ipsen. **S.M.** discloses employment with Genentech.

Correspondence and requests for materials should be addressed to Thomas Powles, M.D., and Sanjeev Mariathasan, Ph.D. Reprints and permissions information is available at www.nature.com/reprints.

Funding information:

The study was sponsored by F. Hoffmann-La Roche Ltd./Genentech, Inc., a member of the Roche Group.

Data availability:

The data required to reproduce results, including figures and tables, will be made available upon request. Qualified researchers may request access to individual patient level data through the

clinical study data request platform (https://vivli.org/). Further details on Roche's criteria for eligible studies are available here (https://vivli.org/members/ourmembers/). For further details on Roche's Global Policy on the Sharing of Clinical Information and how to request access to related clinical study documents, see here (https://www.roche.com/research_and_development/who_we_are_how_we_work/clinical_trials/our_commitment_to_data_sharing.htm).

Code availability statement

Fully documented code for the R statistical computing environment will be provided on request to reproduce the figures and tables.

References

1 Chin, R. I. *et al.* Detection of Solid Tumor Molecular Residual Disease (MRD) Using Circulating Tumor DNA (ctDNA). *Mol Diagn Ther* **23**, 311-331, doi:10.1007/s40291-019-00390-5 (2019).

2 Coakley, M., Garcia-Murillas, I. & Turner, N. C. Molecular Residual Disease and Adjuvant Trial Design in Solid Tumors. *Clinical Cancer Research* **25**, 6026-6034, doi:10.1158/1078-0432.Ccr-19-0152 (2019).

3 Dasari, A. *et al.* ctDNA applications and integration in colorectal cancer: an NCI Colon and Rectal–Anal Task Forces whitepaper. *Nature Reviews Clinical Oncology*, doi:10.1038/s41571-020-0392-0 (2020).

4 Christensen, E. *et al.* Early Detection of Metastatic Relapse and Monitoring of Therapeutic Efficacy by Ultra-Deep Sequencing of Plasma Cell-Free DNA in Patients With Urothelial Bladder Carcinoma. *J Clin Oncol* **37**, 1547-1557, doi:10.1200/JCO.18.02052 (2019).

5 Mok, T. *et al.* Detection and Dynamic Changes of EGFR Mutations from Circulating Tumor DNA as a Predictor of Survival Outcomes in NSCLC Patients Treated with First-line Intercalated Erlotinib and Chemotherapy. *Clin Cancer Res* **21**, 3196-3203, doi:10.1158/1078-0432.CCR-14-2594 (2015).

6 Tie, J. *et al.* Circulating tumor DNA analysis detects minimal residual disease and predicts recurrence in patients with stage II colon cancer. *Sci Transl Med* **8**, 346ra392, doi:10.1126/scitranslmed.aaf6219 (2016).

7 Garcia-Murillas, I. *et al.* Assessment of Molecular Relapse Detection in Early-Stage Breast Cancer. *JAMA Oncol* **5**, 1473-1478, doi:10.1001/jamaoncol.2019.1838 (2019).

8 Maia, M. C. *et al.* Association of Circulating Tumor DNA (ctDNA) Detection in Metastatic Renal Cell Carcinoma (mRCC) with Tumor Burden. *Kidney Cancer* **1**, 65-70, doi:10.3233/KCA-170007 (2017).

9 Abbosh, C. *et al.* Phylogenetic ctDNA analysis depicts early-stage lung cancer evolution. *Nature* **545**, 446-451, doi:10.1038/nature22364 (2017).

10 Chaudhuri, A. A. *et al.* Early Detection of Molecular Residual Disease in Localized Lung Cancer by Circulating Tumor DNA Profiling. *Cancer Discov* **7**, 1394-1403, doi:10.1158/2159-8290.CD-17-0716 (2017).

11 Velimirovic, M. *et al.* Rising Circulating Tumor DNA As a Molecular Biomarker of Early Disease Progression in Metastatic Breast Cancer. *JCO Precision Oncology*, 1246-1262, doi:10.1200/po.20.00117 (2020).

12 Diehl, F. *et al.* Circulating mutant DNA to assess tumor dynamics. *Nature Medicine* **14**, 985-990, doi:10.1038/nm.1789 (2008).

13 Todenhofer, T., Struss, W. J., Seiler, R., Wyatt, A. W. & Black, P. C. Liquid Biopsy-Analysis of Circulating Tumor DNA (ctDNA) in Bladder Cancer. *Bladder Cancer* **4**, 19-29, doi:10.3233/BLC-170140 (2018).

14 Thomsen, M. B. H. *et al.* Comprehensive multiregional analysis of molecular heterogeneity in bladder cancer. *Sci Rep* **7**, 11702, doi:10.1038/s41598-017-11291-0 (2017).

15 Gerlinger, M. *et al.* Intratumor heterogeneity and branched evolution revealed by multiregion sequencing. *N Engl J Med* **366**, 883-892, doi:10.1056/NEJMoa1113205 (2012).

16 Snyder, A., Morrissey, M. P. & Hellmann, M. D. Use of Circulating Tumor DNA for Cancer Immunotherapy. *Clin Cancer Res* **25**, 6909-6915, doi:10.1158/1078-0432.CCR-18-2688 (2019).
17 Gandara, D. R. *et al.* Blood-based tumor mutational burden as a predictor of clinical benefit in non-small-cell lung cancer patients treated with atezolizumab. *Nat Med* **24**, 1441-1448, doi:10.1038/s41591-018-0134-3 (2018).
18 Herbst, R. S. *et al.* Atezolizumab for First-Line Treatment of PD-L1-Selected Patients with NSCLC. *N Engl J Med* **383**, 1328-1339, doi:10.1056/NEJMoa1917346 (2020).
19 Corcoran, R. B. & Chabner, B. A. Application of Cell-free DNA Analysis to Cancer Treatment. *N Engl J Med* **379**, 1754-1765, doi:10.1056/NEJMra1706174 (2018).
20 Turner, N. C. *et al.* Circulating tumour DNA analysis to direct therapy in advanced breast cancer (plasmaMATCH): a multicentre, multicohort, phase 2a, platform trial. *Lancet Oncol* **21**, 1296-1308, doi:10.1016/s1470-2045(20)30444-7 (2020).
21 Tan, M. P., Attard, G. & Huddart, R. A. Circulating Tumour DNA in Muscle-Invasive Bladder Cancer. *Int J Mol Sci* **19**, doi:10.3390/ijms19092568 (2018).
22 Bratman, S. V. *et al.* Personalized circulating tumor DNA analysis as a predictive biomarker in solid tumor patients treated with pembrolizumab. *Nature Cancer* **1**, 873-881, doi:10.1038/s43018-020-0096-5 (2020).
23 Nabet, B. Y. *et al.* Noninvasive Early Identification of Therapeutic Benefit from Immune Checkpoint Inhibition. *Cell*, doi:10.1016/j.cell.2020.09.001 (2020).
24 Moding, E. J., Diehn, M. & Wakelee, H. A. Circulating tumor DNA testing in advanced non-small cell lung cancer. *Lung Cancer* **119**, 42-47, doi:10.1016/j.lungcan.2018.02.019 (2018).
25 Zhang, Q. *et al.* Prognostic and predictive impact of circulating tumor DNA in patients with advanced cancers treated with immune checkpoint blockade. *Cancer Discovery*, CD-20-0047, doi:10.1158/2159-8290.Cd-20-0047 (2020).
26 Kurtz, D. M. *et al.* Circulating Tumor DNA Measurements As Early Outcome Predictors in Diffuse Large B-Cell Lymphoma. *Journal of Clinical Oncology* **36**, 2845-2853, doi:10.1200/jco.2018.78.5246 (2018).
27 Moding, E. J. *et al.* Circulating tumor DNA dynamics predict benefit from consolidation immunotherapy in locally advanced non-small-cell lung cancer. *Nature Cancer* **1**, 176-183, doi:10.1038/s43018-019-0011-0 (2020).
28 Chan, A. T. C. *et al.* Analysis of Plasma Epstein-Barr Virus DNA in Nasopharyngeal Cancer After Chemoradiation to Identify High-Risk Patients for Adjuvant Chemotherapy: A Randomized Controlled Trial. *J Clin Oncol* **36**, 3091-3100, doi:10.1200/JCO.2018.77.7847 (2018).
29 Taieb, J. *et al.* Analysis of circulating tumour DNA (ctDNA) from patients enrolled in the IDEA-FRANCE phase III trial: Prognostic and predictive value for adjuvant treatment duration. *Ann Oncol* **29**, 1211-1219 (2019).
30 Bellmunt, J. *et al.* Adjuvant atezolizumab versus observation in muscle-invasive urothelial carcinoma (IMvigor010): a multicentre, open-label, randomised, phase 3 trial. *Submitted* (2020).
31 Balar, A. V. *et al.* Atezolizumab as first-line treatment in cisplatin-ineligible patients with locally advanced and metastatic urothelial carcinoma: a single-arm, multicentre, phase 2 trial. *Lancet* **389**, 67-76, doi:10.1016/S0140-6736(16)32455-2 (2017).

32 Rosenberg, J. E. *et al.* Atezolizumab in patients with locally advanced and metastatic urothelial carcinoma who have progressed following treatment with platinum-based chemotherapy: a single-arm, multicentre, phase 2 trial. *Lancet* **387**, 1909-1920, doi:10.1016/S0140-6736(16)00561-4 (2016).

33 Horn, L. *et al.* First-Line Atezolizumab plus Chemotherapy in Extensive-Stage Small-Cell Lung Cancer. *N Engl J Med* **379**, 2220-2229, doi:10.1056/NEJMoa1809064 (2018).

34 Gutzmer, R. *et al.* Atezolizumab, vemurafenib, and cobimetinib as first-line treatment for unresectable advanced BRAF(V600) mutation-positive melanoma (IMspire150): primary analysis of the randomised, double-blind, placebo-controlled, phase 3 trial. *Lancet* **395**, 1835-1844, doi:10.1016/S0140-6736(20)30934-X (2020).

35 Finn, R. S. *et al.* Atezolizumab plus Bevacizumab in Unresectable Hepatocellular Carcinoma. *N Engl J Med* **382**, 1894-1905, doi:10.1056/NEJMoa1915745 (2020).

36 Stein, J. P. *et al.* Radical cystectomy in the treatment of invasive bladder cancer: long-term results in 1,054 patients. *J Clin Oncol* **19**, 666-675, doi:10.1200/JCO.2001.19.3.666 (2001).

37 Stenzl, A. *et al.* The updated EAU guidelines on muscle-invasive and metastatic bladder cancer. *Eur Urol* **55**, 815-825, doi:10.1016/j.eururo.2009.01.002 (2009).

38 Coombes, R. C. *et al.* Personalized Detection of Circulating Tumor DNA Antedates Breast Cancer Metastatic Recurrence. *Clinical Cancer Research* **25**, 4255-4263, doi:10.1158/1078-0432.Ccr-18-3663 (2019).

39 Reinert, T. *et al.* Analysis of Plasma Cell-Free DNA by Ultradeep Sequencing in Patients With Stages I to III Colorectal Cancer. *JAMA Oncol*, doi:10.1001/jamaoncol.2019.0528 (2019).

40 Powles, T. *et al.* Atezolizumab versus chemotherapy in patients with platinum-treated locally advanced or metastatic urothelial carcinoma (IMvigor211): a multicentre, open-label, phase 3 randomised controlled trial. *Lancet* **391**, 748-757, doi:10.1016/S0140-6736(17)33297-X (2018).

41 Subramanian, A. *et al.* Gene set enrichment analysis: a knowledge-based approach for interpreting genome-wide expression profiles. *Proc Natl Acad Sci U S A* **102**, 15545-15550, doi:10.1073/pnas.0506580102 (2005).

42 Hellmann, M. D. *et al.* Nivolumab plus Ipilimumab in Lung Cancer with a High Tumor Mutational Burden. *N Engl J Med* **378**, 2093-2104, doi:10.1056/NEJMoa1801946 (2018).

43 Reck, M. *et al.* Pembrolizumab versus Chemotherapy for PD-L1-Positive Non-Small-Cell Lung Cancer. *N Engl J Med* **375**, 1823-1833, doi:10.1056/NEJMoa1606774 (2016).

44 Mariathasan, S. *et al.* TGFbeta attenuates tumour response to PD-L1 blockade by contributing to exclusion of T cells. *Nature* **554**, 544-548, doi:10.1038/nature25501 (2018).

45 Robertson, A. G. *et al.* Comprehensive Molecular Characterization of Muscle-Invasive Bladder Cancer. *Cell* **171**, 540-556 e525, doi:10.1016/j.cell.2017.09.007 (2017).

46 Nuzzo, P. V. *et al.* Detection of urothelial carcinoma using plasma cell-free methylated DNA. *Journal of Clinical Oncology* **38**, 5046-5046 (2020).

47 Nuzzo, P. V. *et al.* Detection of renal cell carcinoma using plasma and urine cell-free DNA methylomes. *Nat Med* **26**, 1041-1043, doi:10.1038/s41591-020-0933-1 (2020).

48 Tan, L. *et al.* Prediction and monitoring of relapse in stage III melanoma using circulating tumor DNA. *Ann Oncol* **30**, 804-814, doi:10.1093/annonc/mdz048 (2019).

49 Wu, T. D. & Nacu, S. Fast and SNP-tolerant detection of complex variants and splicing in short reads. *Bioinformatics* **26**, 873-881, doi:10.1093/bioinformatics/btq057 (2010).
50 Wu, T. D., Reeder, J., Lawrence, M., Becker, G. & Brauer, M. J. GMAP and GSNAP for Genomic Sequence Alignment: Enhancements to Speed, Accuracy, and Functionality. *Methods Mol Biol* **1418**, 283-334, doi:10.1007/978-1-4939-3578-9_15 (2016).
51 Wu, D. & Smyth, G. K. Camera: a competitive gene set test accounting for inter-gene correlation. *Nucleic Acids Res* **40**, e133, doi:10.1093/nar/gks461 (2012).

Methods

Trial Design, Participants, and Endpoints

IMvigor010 was a global, Phase III, open-label, randomised trial of atezolizumab as adjuvant treatment of patients with high-risk MIUC of either the bladder or upper tract (capped at 10%). Inclusion criteria required patients to be high-risk at pathologic staging (pT3-T4a or N+ for patients not treated with neoadjuvant chemotherapy, or pT2-T4a or N+ for patients treated with neoadjuvant chemotherapy). Patients were required to have undergone surgical resection (cystectomy or nephroureterectomy) with lymph node dissection, with no evidence of residual disease or metastasis as confirmed by negative postoperative radiologic imaging.

Patients were randomised 1:1 to either atezolizumab or observation arms. Treatment with atezolizumab (1200 mg every 3 weeks) was administered (or patients underwent observation) for 1 year or until UC recurrence or unacceptable toxicity. Imaging assessments for disease recurrence were performed at baseline and every 12 weeks for 3 years, every 24 weeks for years 4-5, and at year 6. Disease recurrence assessments for patients in the observation arm followed the same schedule as those in the atezolizumab arm. Crossover was not permitted.

The primary efficacy endpoint of IMvigor010 was DFS, which was defined by local (pelvic) or urinary tract recurrence, distant UC metastasis or death from any cause. OS, defined by the time

from randomization to death from any cause, was a secondary efficacy endpoint. The clinical cutoff date was November 30, 2019. At the data cutoff, OS follow-up was immature and ongoing in the ITT population. The median OS was not reached in the interim analysis; 118 patients (29.1%) in the atezolizumab arm and 124 patients in the observation arm (30.8%) died. 33.3% and 29.6% of patients who relapsed received subsequent cancer therapy in the atezolizumab and observation arm respectively. This included chemotherapy in 25.6 and 24.3% respectively and immune therapy in 8.6% and 20.3% respectively and represents treatment patterns for front line advanced disease.

Blood Collection and Processing

The C1D1 plasma timepoint was collected at a median of 79 days post-surgical resection (IQR 65-92 days for MIBC patients). Peripheral blood mononuclear cells (PBMC) were collected in three 8.5-mL acid citrate dextrose tubes at the beginning of C1D1, and peripheral blood plasma was collected in two 6-mL EDTA tubes at the beginning of C1D1 and C3D1. Plasma was separated from the cell pellet within 30 minutes of collection and aliquoted for storage at −80°C. Note that the Natera assay used in this study is validated for frozen plasma utilizing spun-down K2-EDTA collected blood samples within 2 hours of collection, however the clinical version of the assay utilises Streck collection tubes that stabilise cfDNA and allow for ambient shipment within 7 days. A total of 1076 plasma samples (581 from C1D1, 495 from C3D1) from 591 patients were used in this analysis with medians of 3.7 mL plasma used (IQR 3.2-4.2mL) and 21.5 ng cfDNA extracted (IQR 13.2–34.2ng) per patient. To identify ctDNA in a patient's plasma, cfDNA extraction and library prep steps were performed as described previously.[39]

Tumour Tissue Processing

Tumour tissue was collected from surgical resection samples. Genomic DNA was extracted using the QIAamp DNA FFPE Tissue Kit. Central evaluation for PD-L1 expression was conducted using the VENTANA SP142 IHC assay. Tumours were classified as expressing PD-L1 (IC2/3 status) when PD-L1–expressing tumour-infiltrating immune cells covered ≥ 5% of the tumour area.

Whole Exome Sequencing of Tumour Tissue and Matched Normal DNA

A median of 500 ng of genomic DNA (gDNA) was used for the whole exome sequencing workflow for both tumour and normal sources. An Illumina-adapter based library preparation was performed on this gDNA. Targeted exome capture was then performed using a custom capture probe set that targets ~19,500 genes. These targeted libraries were sequenced on the NovaSeq platform at 2 x 100 bp to achieve the deduplicated on-target average coverage of 180X for tumour tissue and 50X for the associated matched normal sample. FastQ files were prepared using bcl2fastq2 and quality checked using FastQC. Reads were mapped to the human reference genome hg19 using Burrows–Wheeler Alignment tool (v.0.7.12) and quality checked using Picard and MultiQC.

Somatic Variant Calling and Signatera ctDNA Assay Design

Using the input of tumour tissue and matched normal sequencing data, somatic variant calling was performed using a consensus variant calling method developed by Natera. Variants previously reported to be germline in public datasets (1000 Genome project, ExAC, ESP, dbSNP) were filtered out, and other collections were also filtered out. The WES data from paired

tumour and matched normal were first analysed for quality metrics and sample concordance and then processed through a bioinformatics pipeline that allows identification of putative clonal somatic single nucleotide variants. Matched normal sequencing was done to computationally remove putative germline and CHIP mutations. Out of the candidate pool of putative clonal variants specific to the tumour DNA of each patient, a prioritised list of variants were used to design PCR amplicons based on optimised design parameters, ensuring uniqueness in the human genome, amplicon efficiency and primer interaction. TMB was calculated as the total number of somatic mutations per megabase of captured exome, and TMB positive patients were those with ≥10 mutations/Mb (the mean of the ctDNA BEP).

Following plasma cfDNA extraction and library prep, multiplexed targeted PCR was conducted on an aliquot of cfDNA library, followed by amplicon-based sequencing and to an average next-generation sequencing depth per amplicon of >100,000x on an Illumina platform. On observing at least 2 or more mutations in the patient's plasma, the patient was deemed ctDNA(+). Analytical studies of the Natera Signatera assay, as previously published, have demonstrated a >95% sensitivity at 0.01% variant allele frequency with high specificity. The turnaround time for the Signatera assay is (i) 2-3 weeks for the first plasma sample, including tissue WES, assay design, and plasma ctDNA analysis/reporting and (ii) one week for all subsequent plasma processing and ctDNA analysis/reporting.

RNA processing

Formalin-fixed paraffin-embedded (FFPE) tissue was macro-dissected for tumour area using H&E as a guide. RNA was extracted using the High Pure FFPET RNA Isolation Kit (Roche) and assessed by Qubit and Agilent Bioanalyzer for quantity and quality. First strand cDNA synthesis was primed from total RNA using random primers, followed by the generation of second strand cDNA with dUTP in place of dTTP in the master mix to facilitate preservation of strand information. Libraries were enriched for the mRNA fraction by positive selection using a cocktail of biotinylated oligos corresponding to coding regions of the genome. Libraries were sequenced using the Illumina sequencing method.

RNA-seq data generation and processing

Whole-transcriptome profiles were generated using TruSeq RNA Access technology (Illumina). RNA-seq reads were first aligned to ribosomal RNA sequences to remove ribosomal reads. The remaining reads were aligned to the human reference genome (NCBI Build 38) using GSNAP,[49,50] version 2013-10-10, allowing a maximum of two mismatches per 75 base sequence (parameters: '-M 2 -n 10 -B 2 -i 1 -N 1 -w 200000 -E 1-pairmax-rna = 200000 –clip-overlap). To quantify gene expression levels, the number of reads mapped to the exons of each RefSeq gene was calculated using the functionality provided by the R/Bioconductor package GenomicAlignments. Raw counts were adjusted for gene length using transcript-per-million (TPM) normalization, and subsequently log2-transformed. Raw and processed data are available under the data sharing agreement for N=728 patients with RNA-seq data available. All analyses in this study use N=573 patients with both RNA-seq and ctDNA data available.

Unsupervised mRNA expression clustering

TCGA subtypes were assigned according to the methodology described previously.[45] Briefly, RNA expression data *R f*or samples were normalized using trimmed mean of M-values normalization and transformed with voom, resulting in $\log_2$-counts per million with associated precision weights. The top 25% most-varying genes, ranked by standard deviation across all samples considered were selected. The $\log_2$ normalized expression of 4660 genes were median centered before performing consensus clustering, categorizing the samples into five clusters. The expression clustering analysis was done with a consensus hierarchical clustering approach using the distance matrix of $1 - C$, the element C_{ij} representing the Spearman correlation between the sample i and j across 4660 genes in R. A consensus matrix M_K, K=5 being the number of clusters, was computed by iterating a standard hierarchical clustering (K * 500) times with the average linkage option and 80% resampling in sample space. The clustering recapitulated the five distinct clusters as reported in ref 45, as indicated by the signatures shown on the heatmap.

Gene set enrichment analysis (GSEA)

GSEA ranks all of the genes in the dataset based on differential expression. GSEA was performed followed by applying the CAMERA enrichment method[51] to perform a competitive test to assess whether the genes in a given set are highly ranked in terms of differential expression relative to genes that are not in the set. The Hallmark gene set collection from the Molecular Signature Database[41] was used to identify the pathways enriched. Pathways with adjusted P values <0.05 were included.

Statistical Analysis

The ctDNA SAP was planned and finalised before unblinding of clinical data for primary trial analysis. The primary objectives for the ctDNA study were to provide evidence that 1) within the ctDNA(+) patients at C1D1, atezolizumab is associated with increased DFS compared with the observation arm, 2) within each arm, C1D1 ctDNA(+) status is associated with decreased DFS compared with ctDNA(–) status, 3) the clearance of ctDNA in plasma by C3D1 is associated with increased DFS and clearance occurs at a higher rate in atezolizumab arm compared with the observation arm. Clearance is defined in this study as going from ctDNA(+) at C1 to ctDNA(-) at C3, and is assessed only in patients who are ctDNA(+) at C1. Primary analysis first used a univariable approach with categorical ctDNA status (ctDNA+/–), followed by ctDNA as a continuous variable (not shown), and finally a multivariable approach including known risk factors. Secondary endpoints included OS, and secondary biomarkers included PD-L1 and TMB. The analysis plan required significance assessment for primary analyses to be made at a level of p-value < 0.05. However, since no multiplicity adjustment was pre-specified in the SAP or applied to subgroup analyses, all p-values should be interpreted with caution.

HRs for recurrence or death are estimated using a multivariable Cox proportional-hazards model adjusting for nodal status (positive or negative), PD-L1 status (IC0/1 or IC2/3), tumour stage (<T3 or T3/4), prior neoadjuvant chemotherapy (Yes or No), and number of lymph nodes resected (<10 or ≥10). Note that the features adjusted may vary depending on subgroups defined by prognostic features (e.g. nodal positive subgroup does not adjust for node status in the multivariable cox model). Similarly, HRs calculated for subgroups defined by transcriptomic signatures do not adjust for PDL1 status. For completeness, in the Extended Data (Extended Data

Tables 3, 6, 9 and 10) we provide additional estimates for 1) univariable Cox model, and 2) stratified Cox model using the same stratification factors as described for the IMvigor010 primary clinical analysis (nodal status, PD-L1 status, and tumour stage).[30] All Cox models used "exact" method for handling tied event times. DFS and OS were compared between treatment groups using the log-rank test, and Kaplan-Meier methodology was applied to DFS and OS with 95% CIs constructed by Greenwood's formula.

Descriptive statistics were used to summarise clinical characteristics, including the mean, median and range for continuous variables and frequency and percentage for categorical variables. Comparison of ctDNA clearance between arms was assessed using Fisher's Exact test (two-sided). Association between ctDNA positivity and baseline prognostic factors were measured using the Kruskal-Wallis Rank Sum test for numeric variables and Fisher's Exact test (two-sided) for categorical variables. Association between C1D1 collection time in days from surgery and ctDNA status was measured using Wilcoxon test (two-sided). All statistical analyses were performed in R (https://www.R-project.org/).

Fig. Legends

Figure 1 | Kaplan-Meier (KM) estimates among patients evaluated for post-surgical ctDNA status. a, Kaplan-Meier estimates of DFS comparing ctDNA(+) patients treated with atezolizumab (dark blue) and ctDNA(+) patients on the observation arm (dark red) (median 5.9 vs 4.4 months), and comparing ctDNA(–) patients treated with atezolizumab (light blue) and ctDNA(–) patients on the observation arm (light red) (medians not reached), **b,** Kaplan-Meier estimates of interim OS in patients evaluated for ctDNA status, comparing ctDNA(+) patients treated with atezolizumab (dark blue) and ctDNA(+) patients on the observation arm (dark red) (median 25.8 vs 15.8 months), and comparing ctDNA(–) patients treated with atezolizumab (light blue) and ctDNA(–) patients on the observation arm (light red) (medians not reached). **c,** Forest plot for DFS in biomarker evaluable population comparing atezolizumab versus observation in subgroups defined by established prognostic factors. **d,** Forest plot for OS in biomarker evaluable population comparing atezolizumab versus observation in subgroups defined by established prognostic factors. MST refers to median survival time in months. **e,** Bar plot depicting association of baseline prognostic factors with ctDNA status.

Figure 2 | Changes in ctDNA status from baseline (C1D1) to on-treatment (C3D1) time point. a, Proportion of patients who are ctDNA(+) at C1D1 that clear ctDNA by C3D1 for atezolizumab arm (blue) and observation arm (red). **b-e,** Kaplan-Meier analyses showing different ctDNA dynamics from C1D1 to C3D1 including patients who were ctDNA(+) at C1D1 and cleared ctDNA by C3D1 (Pos>Neg; light solid lines), patients who were ctDNA(+) at C1D1 and did not clear ctDNA (Pos>Pos; light dashed lines), patients who were ctDNA(–) at C1D1 and remained ctDNA(–) at C3D1 (Neg>Neg; dark solid lines), and patients who were ctDNA(–)

at C1D1 and became ctDNA(+) at C3D1 (Neg>Pos; dark dashed line), for **b,** DFS in the atezolizumab arm (blue colors), **c,** OS in the atezolizumab arm (blue colors), **d,** DFS in the observation arm (red colors), and **e,** OS in the observation arm (red colors).

Figure 3 | Transcriptional correlates of ctDNA positivity, and biomarkers for response to atezolizumab within the ctDNA(+) population. a, Differential gene expression analysis showing genes associated with ctDNA positivity and ctDNA negativity. **b,** Hallmark gene set enrichment analysis showing pathways associated with ctDNA positivity (red) and ctDNA negativity (grey). **c,** Hallmark gene set enrichment analysis showing pathways associated with relapse (red) and non-relapse (blue). **d,** Forest plot for OS in ctDNA(+) population comparing atezolizumab versus observation in subgroups defined by established and/or putative immune biomarkers of response (PDL1, TMB, tGE3) and resistance (TBRs, Angiogenesis) to immunotherapy. MST refers to median survival time in months. **e-i,** Kaplan-Meier analyses for ctDNA(+) patients in the atezolizumab (blue) and observation (red) arms in subgroups defined by immune biomarkers of response to immunotherapy including **e,** PD-L1 by IHC, **f,** TMB from whole exome sequencing, **g,** tGE3 gene expression signature, and subgroups defined by immune biomarkers of resistance to immunotherapy including **h**, pan-TBRS gene expression signature, and **i,** angiogenesis gene expression signature.

Figure 4 | TCGA subtypes and correlates of relapse. a, Heirarchical clustering in ctDNA biomarker evaluable population recapitulates TCGA subtypes for urothelial carcinoma. **b-e**, Kaplan-Meier analyses showing prognostic and/or predictive value of ctDNA status and TCGA subtype in in ctDNA biomarker evaluable population for **b,** Luminal papillary, **c,** Luminal

infiltrated, **d,** Luminal, and **e,** Basal-Squamous. **f,** Forest plot for OS comparing atezolizumab versus observation for TCGA subtypes in ctDNA(-) population (top half) and ctDNA(+) population (bottom half). MST refers to median survival time in months. **g,** Differential gene expression analysis in observation arm ctDNA(-) patients showing genes associated with relapse and non-relapse. **h,** Hallmark gene set enrichment analysis in observation arm ctDNA(-) patients showing pathways associated with relapse (red) and non-relapse (blue). **i**, Barplot in ctDNA(-) patients (arms combined) showing distribution of TCGA subtypes binned by relapse (left) or nonrelapse (right). **j,** Barplot in relapsing patients (arms combined) showing proportion of patients that are ctDNA(+) (red) and ctDNA(−) (blue) binned by either distant relapse or local relapse.

Extended Data Figure Legends

Extended Data Figure 1 | IMvigor010 ctDNA biomarker evaluable population (BEP). a, Inclusion criteria for the ctDNA BEP. Of the 809 patients enrolled in IMvigor010, 581 passed the predetermined quality control criteria. **b-e**, Kaplan-Meier (KM) estimates comparing patients treated with atezolizumab (blue) to observation (red) for **b,** DFS in the ITT population, stratified for nodal status, PD-L1 status, and tumour stage, **c,** DFS in the ctDNA BEP population, stratified for nodal status, PD-L1 status, and tumour stage, **d**, interim OS in the ITT, stratified for nodal status, PD-L1 status, and tumour stage and e, interim OS in the ctDNA BEP population, stratified for nodal status, PD-L1 status, and tumour stage. Formal testing in IMvigor010 of OS survival as the secondary endpoint was not permitted based on the hierarchical study design; thus, the P value is for descriptive purposes only. Note that stratification factors in this analysis were chosen to match exactly those used in IMvigor010 primary clinical analysis.[30]

Extended Data Figure 2 | Continuous ctDNA levels and clinical outcomes within ctDNA(+) patients. Only the observation arm is shown to demonstrate prognostic value of baseline ctDNA. **a,** Scatter plot showing ctDNA level as measured by sample mean mutant tumour molecules per mL of plasma (sample mean MTM) vs DFS in months. Solid points indicate an event, and empty points indicate censoring**. b,** Kaplan-Meier plot for DFS comparing patients with high ctDNA levels (blue, greater than or equal to median sample mean MTM) versus low ctDNA levels (red, less than the median sample mean MTM) **c,** Forest plot for DFS comparing patients with high versus low ctDNA levels using different quantile thresholds for splitting sample mean MTM, including a 10% quantile, 25% quantile, 50% (median) quantile, 75% quantile, and 90% quantile. **d,** Scatter plot showing OS in months (x-axis) versus ctDNA level as measured by sample mean MTM. Solid points indicate an event, and empty points indicate censoring. **e**, Kaplan-Meier plot for OS comparing patients with high ctDNA levels (dark red, greater than or equal to median sample mean MTM) versus low ctDNA levels (light red, less than the median sample mean MTM). f, Forest plot for OS comparing patients with high versus low ctDNA levels using different quantile thresholds for splitting ctDNA sample mean MTM, including a 10% quantile, 25% quantile, 50% (median) quantile, 75% quantile, and 90% quantile.

Extended Data Figure 3 | ctDNA and C1D1 collection time and time until relapse. Note that collection time analyses are shown for patients with muscle-invasive bladder cancer only, because patients with upper-tract urothelial carcinoma often received 2 surgeries. **a,** Scatter plot showing ctDNA levels (sample mean MTM) vs C1D1 collection time (days from surgery). **b,** Box plot showing the C1D1 collection time (y-axis) for the ctDNA negative (x-axis, left box plot) and ctDNA positive (x-axis, right box plot) patients. No difference was found between the collection times for the ctDNA negative patients and ctDNA positive patients (Wilcoxon p=0.18). **c,** Bar plot showing the fraction of patients who were ctDNA positive (red fill) for patients with C1D1 collection times less than the median collection time (x-axis, left bar plot) and greater than the median collection time (x-axis, right bar plot). **d,** Histogram showing the distribution of times between surgery and C1D. **e,** Histogram plot showing the distribution of durations between a C1D1 ctDNA(+) test and radiological relapse.

Extended Data Figure 4 | Reductions in ctDNA levels occurred at a higher rate in the atezolizumab arm compared with the observation arm and were associated with

improvements in clinical outcome in the atezolizumab arm. Reduction is assessed in C1D1 ctDNA+ patients in the C1/C3 BEP and is defined as a decrease in sample mean MTM from C1 to C3 **a,** Proportion of patients who are ctDNA(+) at C1D1 that have reduced ctDNA by C3D1 for the atezolizumab arm (blue) and the observation arm (red). **b-e.** Kaplan-Meier analyses comparing patients who have reduced ctDNA (reduction or clearance, dark blue or dark red) compared with those who have ctDNA levels that remain the same or increase ('non-reduction', light blue or light red) for **b,** DFS in the atezolizumab arm, **c,** DFS in the observation arm, **d,** OS in the atezolizumab arm, and **e,** OS in the observation arm.

Extended Data Figure 5 | Patients who clear ctDNA with atezolizumab have better outcomes than patients who have reductions in ctDNA without clearance. Patients shown are from the atezolizumab arm C1/C3 BEP and are ctDNA+ at baseline and have different types of ctDNA dynamics based on the percent change in sample mean MTM from C1 to C3. Note that the scale for percent change goes from −100% (clearance) to infinity, where negative values indicate reductions, and positive values indicate increases. Kaplan-Meier analysis of **a,** DFS and **c,** OS wherein ctDNA reduction is split into patients who clear ctDNA ('reduction with clearance', dark blue, solid lines) and those who have decreased ctDNA without clearance ('reduction without clearance', dark blue, dashed lines). Patients with an increase in ctDNA are also shown ('increase', light blue, solid lines). Forest plots for **b,** DFS and **d,** comparing patients with reduction (anywhere from clearance (−100% change) to minor decreases in ctDNA (<0% change)) using different thresholds for percent change in sample mean MTM, including −100% change (reduction with clearance versus reduction without clearance), −50% change, −25% change, and −10% change.

Extended Data Figure 6 | Forest plots for OS in subgroups defined by ctDNA status and clinical or immune features. Forestplots for OS in ctDNA populations comparing atezolizumab to observation including **a**, all ctDNA evaluable patients, **b**, ctDNA(–) patients, **c,** ctDNA(+) patients. Subgroups defined by baseline clinical features and tissue immune biomarkers including nodal status, tumor stage, prior neoadjuvant, PDL1 status by IHC, TMB status by WES, as well as transcriptomic signatures including tGE3, TBRs, Angiogenesis, and TCGA subtypes. MST refers to median survival time in months.

Extended Data Figure 7 | Forest plots for DFS in subgroups defined by ctDNA status and clinical or immune features. Forestplots for OS in ctDNA populations comparing atezolizumab to observation including **a**, all ctDNA evaluable patients, **b**, ctDNA(–) patients, **c,** ctDNA(+) patients. Subgroups defined by baseline clinical features and tissue immune biomarkers including nodal status, tumor stage, prior neoadjuvant, PDL1 status by IHC, TMB status by WES, as well as transcriptomic signatures including tGE3, TBRs, Angiogenesis, and TCGA subtypes. MST refers to median survival time in months.

Extended Data Figure 8 | Exploring predictive biomarkers for response to atezolizumab in ctDNA(+) populations. a-e, Kaplan-Meier analyses for ctDNA(+) patients in the atezolizumab (blue) and observation (red) arms in subgroups defined by immune biomarkers of response to immunotherapy including **a,** PD-L1 by IHC, **b,** TMB from whole exome sequencing, **c,** tGE3 gene expression signature, and subgroups defined by immune biomarkers of resistance to immunotherapy including **d,** pan-TBRS gene expression signature, and **e,** angiogenesis gene

expression signature. **f,** Hallmark gene set enrichment analysis in ctDNA+ patients in the observation arm comparing non-relapsers (blue) to relapsers (red).

Extended Data Figure 9 | Tissue biomarkers in ctDNA(−) patients. Kaplan-Meier curves for ctDNA(−) patients for DFS (left) and OS (right) for PDL1 status by IHC, TMB status by WES, and transcriptomic signatures including tGE3, TBRs, and Angiogenesis.

Extended Data Figure 10 | Triple positive patients (ctDNA+/PDL1+/TMB+) have improved outcomes with atezolizumab compared to observation. Patients shown are those who are ctDNA+ at baseline and evaluable for ctDNA and TMB status. 'Triple positive' is defined as ctDNA+/TMB+/PDL1+, whereas 'not triple positive' is defined as those who are either single positive (ctDNA+) or double positive with ctDNA (ctDNA+ and either TMB+ or PDL1+). Kaplan-Meier estimates are shown for a, DFS in triple-positive patients, **b,** DFS in non–triple-positive patients, **c,** OS in triple-positive patients, and **d,** OS in non–triple-positive patients.

Extended Data Figure 11 | TCGA subgroups and DFS Kaplan-Meier analyses. (a) TCGA subgroups are similarly distributed in ctDNA+ and ctDNA− populations. (b) TCGA subgroup distribution is associated with PDL1 status. (c-f) Kaplan-Meier analyses for DFS showing ctDNA+ (dark colors) and ctDNA− (light colors) patients on atezolizumab (blue) and observation (red) for TCGA subgroups. (g-h) Kaplan-Meier analyses for DFS and OS in neuronal TCGA subgroup.

Extended Data Tables

Extended Data Table 1 | Comparison of baseline characteristics in the intention-to-treat and Cycle 1 Day 1 biomarker-evaluable populations

Characteristic	Intention-to-Treat Population		Biomarker-Evaluable Population	
	Atezolizumab (n=406)	Observation (n=403)	Atezolizumab (n=300)	Observation (n=281)
Median age (range) — yr	67 (31–86)	66 (22–88)	67 (31–85)	66 (37–88)
Race — no. (%)				
White	320 (78.8%)	307 (76.2%)	242 (80.7%)	220 (78.3%)
Asian	64 (15.8%)	68 (16.9%)	42 (14.1%)	42 (15.0%)
Black or African American	3 (0.7%)	3 (0.7%)	2 (0.7%)	1 (0.4%)
Other	6 (1.5%)	4 (1.0%)	6 (2.0%)	3 (1.1%)
Unknown	12 (3.0%)	21 (5.2%)	7 (2.3%)	15 (5.3%)
Sex — no. (%)				
Female	84 (20.7%)	87 (21.6%)	67 (22.3%)	62 (21.4%)
Male	322 (79.3%)	316 (78.4%)	233 (77.7%)	221 (78.7%)
Baseline Eastern Cooperative Oncology Group performance score — no. (%)				
0	248 (61.1%)	259 (64.3%)	188 (62.7%)	183 (65.1%)
1	142 (35.0%)	130 (32.3%)	99 (33.0%)	88 (31.3%)
2	16 (3.9%)	14 (3.5%)	13 (4.3%)	10 (3.6%)
Primary tumour site — no. (%)				
Muscle-invasive bladder cancer	377 (92.9%)	378 (93.8%)	278 (92.7%)	260 (92.5%)
Upper tract urothelial carcinoma	29 (7.1%)	25 (6.2%)	22 (7.3%)	21 (7.4%)
Tumour stage — no. (%)				
<PT2/PT2	104 (25.6%)	101 (25.1%)	77 (25.7%)	71 (25.3%)
PT3/PT4	302 (74.4%)	302 (74.9%)	223 (74.3%)	210 (74.7%)
Prior neoadjuvant or adjuvant treatment — no. (%)				
No	210 (51.7%)	214 (53.1%)	154 (51.3%)	147 (52.3%)
Yes	196 (48.3%)	189 (46.9%)	146 (48.7%)	134 (47.7%)
PD-L1 status* — no. (%)				
IC0/1: PD-L1(–)	210 (51.7%)	207 (51.4%)	160 (53.3%)	145 (51.9%)
IC2/3: PD-L1(+)	196 (48.3%)	196 (48.6%)	140 (46.7%)	136 (48.1%)
Lymph nodes — no. (%)				
<10	95 (23.4%)	94 (23.3%)	65 (21.7%)	62 (22.1%)
≥10	311 (76.6%)	309 (76.7%)	235 (78.3%)	219 (77.9%)
Nodal status — no. (%)				
Negative	194 (47.8%)	195 (48.4%)	145 (48.3%)	133 (47.3%)
Positive	212 (52.2%)	208 (51.6%)	155 (51.7%)	148 (52.7%)
Median TMB (range), mut/mb	6.89 (0.51–268.80)†	7.05 (0.41–262.63)‡	6.75 (0.51–52.73)	7.02 (0.41–73.52)

* Per VENTANA SP142 immunohistochemistry assay. †Eighty-five patients had missing data. ‡One hundred nine patients had missing data.

Extended Data Table 2 | Comparison of baseline characteristics between treatment arms in the C1D1 biomarker–evaluable population (BEP)

n (%)	Atezolizumab (n=300)	Observation (n=281)	*P* value
Cycle 1 Day 1 ctDNA status — no. (%)			0.39
Negative	184 (61.3%)	183 (65.1%)	
Positive	116 (38.7%)	98 (34.9%)	
Median age (range) — yr	67 (31–85)	66 (37–88)	0.89
Race — no. (%)			0.31
White	242 (80.7%)	220 (78.3%)	
Asian	42 (14.0%)	42 (1.50%)	
Black or African American	2 (0.7%)	1 (0.4%)	
Other	6 (2.0%)	3 (1.1%)	
Unknown	7 (2.3%)	15 (5.3%)	
Sex — no. (%)			0.84
Female	67 (22.3%)	60 (21.4%)	
Male	233 (77.7%)	221 (78.7%)	
Baseline Eastern Cooperative Oncology Group performance score — no. (%)			0.79
0	188 (62.7%)	183 (65.1%)	
1	99 (33.0%)	88 (31.3%)	
2	13 (4.3%)	10 (3.6%)	
Primary tumour site — no. (%)			>0.99
Muscle-invasive bladder cancer	278 (92.7%)	260 (92.5%)	
Upper tract urothelial carcinoma	22 (7.3%)	21 (7.5%)	
Tumour stage — no. (%)			0.92
<PT2/PT2	77 (25.7%)	71 (25.3%)	
PT3/PT4	223 (74.3%)	210 (74.7%)	
Prior neoadjuvant or adjuvant treatment — no. (%)			0.87
No	154 (51.3%)	147 (52.3%)	
Yes	146 (48.7%)	134 (47.7%)	
PD-L1 status* — no. (%)			0.68
IC0/1: PD-L1(–)	160 (53.3%)	145 (51.6%)	
IC2/3: PD-L1(+)	140 (46.7%)	136 (48.4%)	
Lymph nodes — no. (%)			0.92
<10	65 (21.7%)	62 (22.1%)	
≥10	235 (78.3%)	219 (77.9%)	
Nodal status — no. (%)			0.87
Negative	145 (48.3%)	133 (47.3%)	
Positive	155 (51.7%)	148 (52.7%)	
Median TMB (range), mut/Mb	6.75 (0.51–52.73)	7.02 (0.41–73.52)	0.45

* Per VENTANA SP142 immunohistochemistry assay.

Extended Data Table 3 | DFS and OS: ctDNA(+) vs ctDNA(–) for atezolizumab and observation arms

Model	DFS HR (95% CI)	OS HR (95% CI)	No. of patients
Atezolizumab arm: C1D1 ctDNA(+) vs C1D1 ctDNA(–)			ctDNA(–): 184 ctDNA(+): 116 Total: 300
Univariate*	3.36 (2.44–4.62)	3.63 (2.34–5.64)	
IMvigor010 primary†	3.56 (2.51–5.04)	4.19 (2.61–6.73)	
Multivariate‡	3.39 (2.43–4.47)	4.08 (2.57–6.47)	
Observation: C1D1 ctDNA(+) vs C1D1 ctDNA(–)			ctDNA(–): 183 ctDNA(+): 98 Total: 281
Univariate	6.30 (4.45–8.92)	8.00 (4.92–12.99)	
IMvigor010 primary	6.27 (4.32–9.09)	8.08 (4.83–13.51)	
Multivariate	6.19 (4.29–8.91)	7.92 (4.81–13.05)	
Atezolizumab arm: C3D1 ctDNA(+) vs C3D1 ctDNA(–)			ctDNA(–): 170 ctDNA(+): 93 Total: 263
Univariate	5.24 (3.68–7.45)	6.00 (3.6–10.00)	
IMvigor010 primary	5.87 (3.99–8.63)	7.35 (4.26–12.69)	
Multivariate	5.37 (3.73–7.74)	6.94 (4.08–11.82)	
Observation arm: C3D1 ctDNA(+) vs C3D1 ctDNA(–)			ctDNA(–): 129 ctDNA(+): 93 Total: 222
Univariate	8.65 (5.67–13.18)	12.74 (6.26–25.93)	
IMvigor010 primary	8.10 (5.15–12.76)	12.07 (5.63–25.86)	
Multivariate	8.36 (5.35–13.07)	11.80 (5.67–24.48)	

C1D1 ctDNA status based on C1D1 BEP. C3D1 ctDNA status based on C1/C3 BEP.
* Univariate Cox proportional-hazard model was prespecified in ctDNA statistical analysis plan. † Stratified Cox proportional-hazards model was used for IMvigor010 primary analysis. Stratification factors were: nodal status (+ or –), PD-L1 status (IC0/1 or IC2/3), and tumour stage (≤ pT2 or pT3/4). ‡ Multivariable Cox proportional-hazards regression analysis was prespecified in ctDNA statistical analysis plan. Stratification factors were: nodal status (+ or –), PD-L1 status (IC0/1 or IC2/3), tumour stage (≤ pT2 or pT3/4), prior neoadjuvant chemotherapy (yes or no), and number of lymph nodes (<10 or ≥10).

Extended Data Table 4 | Prognostic factors associated with ctDNA status at C1D1.

n (%)	ctDNA(+) (n=214)	ctDNA(–) (n=367)	P value
Median age (range) — yr	67 (32-88)	66 (31-85)	0.30
Race — no. (%)			0.31
White	172 (80.4%)	290 (79.0%)	
Asian	27 (12.6%)	57 (15.5%)	
Black or African American	0	3 (0.8%)	
Other	3 (1.4%)	6 (1.6%)	
Unknown	12 (5.6%)	10 (2.7%)	
Sex — no. (%)			0.30
Female	52 (24.3%)	75 (20.4%)	
Male	162 (75.7%)	292 (79.6%)	
Baseline Eastern Cooperative Oncology Group performance score — no. (%)			0.30
0	135 (63.1%)	236 (64.3%)	
1	67 (31.3%)	120 (32.7%)	
2	12 (5.6%)	11 (3.0%)	
Primary tumour site — no. (%)			0.87
Muscle-invasive bladder cancer	199 (93.0%)	339 (92.4%)	
Upper tract urothelial carcinoma	15 (7.0%)	28 (7.6%)	
Tumour stage — no. (%)			0.09
<PT2/PT2	46 (21.5%)	102 (27.8%)	
PT3/PT4	168 (78.5%)	265 (72.2%)	
Prior neoadjuvant or adjuvant treatment — no. (%)			>0.99
No	111 (51.9%)	190 (51.8%)	
Yes	103 (48.1%)	177 (48.2%)	
PD-L1 status* — no. (%)			>0.99
PD-L1(–)†	112 (52.3%)	193 (52.6%)	
PD-L1(+)‡	102 (47.7%)	174 (47.4%)	
Lymph nodes — no. (%)			>0.99
<10	47 (22.0%)	80 (21.8%)	
≥10	167 (78.0%)	287 (78.2%)	
Nodal status — no. (%)			<0.001
Negative	70 (32.7%)	208 (56.7%)	
Positive	144 (67.3%)	159 (43.3%)	
Median TMB (range), mut/mb	7.09 (0.41–44.62)	6.63 (0.61–73.52)	0.36

Baseline prognostic factors were studied for association with ctDNA status at C1D1, and nodal positivity was found to correlate with ctDNA positivity. No other features were significantly associated with ctDNA positivity.
* Per VENTANA SP142 immunohistochemistry assay. † PD-L1(–) defined by IC0/1 status: PD-L1–expressing immune cells covering <5% of the tumour area.‡ PD-L1(+) defined by IC2/3 status: PD-L1–expressing immune cells covering ≥5% of the tumour area.

Extended Data Table 5 | Balance of baseline characteristics between arms within ctDNA+ population

	Atezolizumab (n=116)	Observation (n=98)	*P* value
Median age (range) — yr	67 (32–83)	68 (37–88)	0.58
Race — no. (%)			
Asian	16 (13.8%)	11 (11.2%)	0.41
Other	1 (0.9%)	2 (2.0%)	
Unknown	4 (3.4%)	8 (8.2%)	
White	95 (81.9%)	77 (78.6%)	
Sex — no. (%)			>0.99
Female	28 (24.1%)	24 (24.5%)	
Male	88 (75.9%)	74 (75.5%)	
Baseline Eastern Cooperative Oncology Group performance score — no. (%)			0.38
0	71 (61.2%)	64 (65.3%)	
1	36 (31.0%)	31 (31.6%)	
2	9 (7.8%)	3 (3.1%)	
Primary tumour site — no. (%)			0.42
Muscle-invasive bladder cancer	106 (91.4%)	93 (94.9%)	
Upper tract urothelial carcinoma	10 (8.6%)	5 (5.1%)	
Tumour stage — no. (%)NA's			0.87
<PT2/PT2	24 (20.7%)	22 (22.4%)	
PT3/PT4	92 (79.3%)	76 (77.6%)	
Prior neoadjuvant therapy — no. (%)			0.34
NO	64 (55.2%)	47 (48.0%)	
YES	52 (44.8%)	51 (52.0%)	
PD-L1 status — no. (%)			0.07
IC0/1: PD-L1(–)	54 (46.6%)	58 (59.2%)	
IC2/3: PD-L1(+)	62 (53.4%)	40 (40.8%)	
Lymph nodes — no. (%)			>0.99
<10	25 (21.6%)	22 (22.4%)	
≥10	91 (78.4%)	76 (77.6%)	
Nodal status — no. (%)			0.46
Negative	35 (30.2%)	35 (35.7%)	
Positive	81 (69.8%)	63 (64.3%)	
TMB status			>0.99
TMB_high	37 (31.9%)	32 (32.7%)	
TMB_low	79 (68.1%)	66 (67.3%)	

	Atezolizumab (n=114)	Observation (n=98)	*P* value
tGE3 — no. (%)			0.13
High	63 (55.3%)	43 (43.9%)	
Low	51 (44.7%)	55 (56.1%)	
TBRS — no. (%)			0.41
High	52 (45.6%)	51 (52.0%)	
Low	62 (54.4%)	47 (48.0%)	
TCGA subtype — no. (%)			0.39
Basal-squamous	44 (38.6%)	32 (32.7%)	
Luminal	12 (10.5%)	11 (11.2%)	
Luminal-infiltrated	24 (21.1%)	32 (32.7%)	
Luminal-papillary	32 (28.1%)	22 (22.4%)	
Neuronal	2 (1.8%)	1 (1.0%)	
Angiogenesis — no. (%)			0.68
High	54 (47.4%)	50 (51.0%)	
Low	60 (52.6%)	48 (49.0%)	

* Per VENTANA SP142 immunohistochemistry assay.

Extended Data Table 6 | DFS and OS: atezolizumab vs observation based on C1D1 ctDNA status

Model	DFS HR (95% CI)	OS HR (95% CI)	No. of patients
C1D1 ctDNA(+) subgroup: Atezolizumab vs observation			Atezolizumab: 116 Observation: 98 Total: 214
Univariate*		0.59 (0.41–0.86)	
IMvigor010 primary†	0.57 (0.41–0.79)	0.58 (0.39–0.85)	
Multivariate‡	0.56 (0.41–0.77)	0.58 (0.40–0.86)	
C1D1 ctDNA(–) subgroup: Atezolizumab vs observation			Atezolizumab: 184 Observation: 183 Total: 367
Univariate		1.31 (0.77–2.23)	
IMvigor010 primary	1.07 (0.75–1.53)	1.22 (0.71–2.09)	
Multivariate	1.07 (0.75–1.52)	1.22 (0.71–2.08)	

* Univariate Cox proportional-hazard model was prespecified in ctDNA statistical analysis plan. † Stratified Cox proportional-hazards model was used for IMvigor010 primary analysis. Stratification factors were: nodal status (+ or –), PD-L1 status (IC0/1 or IC2/3), and tumour stage (≤ pT2 or pT3/4). ‡ Multivariable Cox proportional-hazards regression analysis was prespecified in ctDNA statistical analysis plan. Stratification factors were: nodal status (+ or –), PD-L1 status (IC0/1 or IC2/3), tumour stage (≤ pT2 or pT3/4), prior neoadjuvant chemotherapy (yes or no), and number of lymph nodes (<10 or ≥10).

Extended Data Table 7 | Comparison of baseline characteristics in the ITT and C1/C3 biomarker-evaluable populations*

Characteristic	ITT Population		C1/C3 BEP	
	Atezolizumab (n=406)	Observation (n=403)	Atezolizumab (n=263)	Observation (n=222)
Median age (range) — yr	67 (31–86)	66 (26–88)	67 (31–85)	66 (37–88)
Race — no. (%)				
White	320 (78.8%)	307 (76.2%)	208 (79.1%)	169 (76.1%)
Non-White	86 (21.2%)	96 (23.8%)	55 (20.9%)	53 (23.9%)
Sex — no. (%)				
Female	84 (20.7%)	87 (21.6%)	60 (22.8%)	51 (23.0%)
Male	322 (79.3%)	316 (78.4%)	203 (77.2%)	171 (77.0%)
Baseline Eastern Cooperative Oncology Group performance score — no. (%)				
0	248 (61.1%)	259 (64.3%)	168 (63.9%)	147 (66.2%)
1	142 (35.0%)	130 (32.3%)	85 (32.3%)	66 (29.7%)
2	16 (3.9%)	14 (3.5%)	10 (3.8%)	9 (4.1%)
Primary tumour site — no. (%)				
Muscle-invasive bladder cancer	377 (92.9%)	378 (93.8%)	244 (92.8%)	204 (91.9%)
Upper tract urothelial carcinoma	29 (7.4%)	25 (6.2%)	19 (7.2%)	18 (8.1%)
Tumour stage — no. (%)				
<PT2/PT2	104 (25.6%)	101 (25.1%)	70 (26.6%)	56 (25.2%)
PT3/PT4	302 (74.38%)	302 (74.94%)	193 (73.38%)	166 (74.77%)
Prior neoadjuvant or adjuvant treatment — no. (%)				
No	210 (51.7%)	214 (53.1%)	134 (51.0%)	115 (51.8%)
Yes	196 (48.3%)	189 (46.9%)	129 (49.1%)	107 (48.2%)
PD-L1 status† — no. (%)				
IC0/1: PD-L1(–)	210 (51.7%)	207 (51.4%)	143 (54.4%)	116 (52.3%)
IC2/3: PD-L1(+)	196 (48.3%)	196 (48.6%)	120 (45.6%)	106 (47.8%)
Lymph nodes — no. (%)				
<10	95 (23.4%)	94 (23.3%)	55 (20.9%)	48 (21.6%)
≥10	311 (76.6%)	309 (76.7%)	208 (79.1%)	174 (78.4%)
Nodal status — no. (%)				
Negative	194 (47.8%)	195 (48.4%)	128 (48.7%)	101 (45.5%)
Positive	212 (52.2%)	208 (51.6%)	135 (51.3%)	121 (54.5%)

*Patients had ctDNA samples at C1 and C3. † Per VENTANA SP142 immunohistochemistry assay.

Extended Data Table 8 | Comparison of baseline characteristics between treatment arms in the C1/C3 BEP

n (%)	Atezolizumab (n=263)	Observation (n=222)	*P* value
ctDNA status at C1D1			0.71
Negative	164 (62.4%)	143 (64.4%)	
Positive	99 (37.6%)	79 (35.6%)	
Median age (range) — yr	66 (31–85)	66 (37–88)	0.59
Race — no. (%)			0.24
White	208 (79.1%)	169 (76.1%)	
Asian	40 (15.2%)	38 (17.1%)	
Black or African American	2 (0.8%)	0	
American Indian or Alaska Native	1 (0.4%)	0	
Other	6 (2.3%)	3 (1.4%)	
Unknown	6 (2.3%)	12 (5.4%)	
Sex — no. (%)			>0.99
Female	60 (22.8%)	51 (23.0%)	
Male	203 (77.2%)	171 (77.0%)	
Baseline Eastern Cooperative Oncology Group performance score — no. (%)			0.84
0	168 (63.9%)	147 (66.2%)	
1	85 (32.3%)	66 (29.7%)	
2	10 (3.8%)	9 (4.1%)	
Primary tumour site — no. (%)			0.73
Muscle-invasive bladder cancer	244 (92.8%)	204 (91.9%)	
Upper tract urothelial carcinoma	19 (7.2%)	18 (8.1%)	
Tumour stage — no. (%)			0.76
<PT2/PT2	70 (26.6%)	56 (25.2%)	
PT3/PT4	193 (73.4%)	166 (74.8%)	
Prior neoadjuvant or adjuvant treatment — no. (%)			0.86
No	134 (51.0%)	115 (51.8%)	
Yes	129 (49.1%)	107 (48.2%)	
PD-L1 status* — no. (%)			0.65
IC0/1: PD-L1(–)	143 (54.4%)	116 (52.3%)	
IC2/3: PD-L1(+)	120 (45.6%)	106 (47.8%)	
Lymph nodes — no. (%)			0.91
<10	55 (20.9%)	48 (21.6%)	
≥10	208 (79.1%)	174 (78.4%)	
Nodal status — no. (%)			0.52
Negative	128 (48.7%)	101 (45.5%)	
Positive	135 (51.3%)	121 (54.5%)	
Median TMB (range), mut/Mb	6.45 (0.51–52.73)	7.05 (0.41–73.52)	

* Per VENTANA SP142 immunohistochemistry assay.

Extended Data Table 9 | DFS and OS: ctDNA clearance vs non-clearance for atezolizumab and observation arms

Model	DFS HR (95% CI)	OS HR (95% CI)	No. of patients
Atezolizumab arm: Clearance vs no clearance			Clearance: 18 No clearance: 81 Total: 99
Univariate*	0.26 (0.12–0.56)	0.41 (0.1–1.70)	
IMvigor010 primary†	0.35 (0.16–0.78)	0.51 (0.12–2.19)	
Multivariate‡	0.32 (0.14–0.71)	0.42 (0.10–1.79)	
Observation arm: Clearance vs no clearance			Clearance: 3 No clearance: 76 Total: 79
Univariate	0.14 (0.03–0.59)	0.66 (0.09–4.81)	
IMvigor010 primary	0.17 (0.04–0.73)	1.15 (0.14–9.41)	
Multivariate	0.17 (0.04–0.72)	1.17 (0.15–9.08)	

Analysis based on patients with C1D1 ctDNA(+) status. * Univariate Cox proportional-hazard model was prespecified in ctDNA statistical analysis plan. † Stratified Cox proportional-hazards model was used for IMvigor010 primary analysis. Stratification factors were: nodal status (+ or –), PD-L1 status (IC0/1 or IC2/3), and tumour stage (≤ pT2 or pT3/4). ‡ Multivariable Cox proportional-hazards regression analysis was prespecified in ctDNA statistical analysis plan. Stratification factors were: nodal status (+ or –), PD-L1 status (IC0/1 or IC2/3), tumour stage (≤ pT2 or pT3/4), prior neoadjuvant chemotherapy (yes or no), and number of lymph nodes (<10 or ≥10).

Extended Data Table 10 | DFS and OS: TMB(+) vs TMB(–) within arms, atezolizumab vs observation with TMB subgroups, and atezolizumab vs observation within subgroups defined by combinations of TMB/ ctDNA status at C1D1

Model	DFS HR (95% CI)	OS HR (95% CI)	No. of patients
Atezolizumab Arm: TMB(–) vs TMB(+)			TMB(–): 207 TMB(+): 93 Total: 300
Univariate*	1.55 (1.08–2.22)	1.62 (0.99–2.66)	
IMvigor010 primary†	1.44 (0.98–2.12)	1.56 (0.93–2.62)	
Multivariate‡	1.36 (0.92–2)	1.48 (0.88–2.48)	
Observation Arm: TMB(–) vs TMB(+)			TMB(–): 181 TMB(+):100 Total: 281
Univariate	1.35 (0.95–1.93)	1.62 (0.99–2.65)	
IMvigor010 primary	1.19 (0.82–1.72)	1.51 (0.91–2.52)	
Multivariate	1.22 (0.84–1.76)	1.46 (0.88–2.43)	
TMB(+) subgroup: Atezolizumab vs observation			Atezolizumab: 93 Observation: 100 Total: 198
Univariate	0.84 (0.55–1.28)	0.92 (0.50–1.67)	
IMvigor010 primary	0.85 (0.54–1.34)	0.86 (0.46–1.61)	
Multivariate	0.89 (0.57–1.38)	0.95 (0.52–1.75)	
TMB(–) subgroup: Atezolizumab vs observation			Atezolizumab: 207 Observation: 181 Total: 388
Univariate	0.94 (0.72–1.23)	0.91 (0.64–1.30)	
IMvigor010 primary	0.89 (0.68–1.17)	0.91 (0.63–1.30)	
Multivariate	0.89 (0.68–1.17)	0.90 (0.63–1.29)	
C1D1 ctDNA(+)/TMB(+) subgroup: Atezolizumab vs observation			Atezolizumab: 37 Observation: 32 Total: 69
Univariate		0.47 (0.22–0.99)	
IMvigor010 primary		0.29 (0.12–0.70)	
Multivariate		0.39 (0.17–0.89)	
C1D1 ctDNA(+)/TMB(–) subgroup: Atezolizumab vs observation			Atezolizumab: 79 Observation: 66 Total: 145
Univariate		0.63 (0.40–0.97)	
IMvigor010 primary		0.68 (0.44–1.07)	
Multivariate		0.65 (0.42–1.01)	
C1D1 ctDNA(–)/TMB(+) subgroup: Atezolizumab vs observation			Atezolizumab: 57 Observation: 68 Total: 125
Univariate		1.54 (0.53–4.45)	
IMvigor010 primary		1.51 (0.44–5.17)	
Multivariate		1.73 (0.56–5.36)	
C1D1 ctDNA(–)/TMB(–) subgroup: Atezolizumab vs observation			Atezolizumab: 128 Observation: 115 Total: 243
Univariate	1.03 (0.69–1.54)	1.19 (0.64–2.20)	
IMvigor010 primary	0.99 (0.65–1.49)	1.19 (0.63–2.23)	
Multivariate	0.94 (0.63–1.42)	1.15 (0.62–2.13)	

* Univariate Cox proportional-hazard model was prespecified in ctDNA statistical analysis plan. † Stratified Cox proportional-hazards model was used for IMvigor010 primary analysis. Stratification factors were: nodal status (+ or –), PD-L1 status (IC0/1 or IC2/3), and tumour stage (≤ pT2 or pT3/4). ‡ Multivariable Cox proportional-hazards regression analysis was prespecified in ctDNA statistical analysis plan. Stratification factors were: nodal status (+ or –), PD-L1 status (IC0/1 or IC2/3), tumour stage (≤ pT2 or pT3/4), prior neoadjuvant chemotherapy (yes or no), and number of lymph nodes (<10 or ≥10).

Extended Data Table 11 | DFS and OS: PD-L1(+) vs PD-L1(–) within arms, atezolizumab vs observation within PD-L1 subgroups, and atezolizumab vs observation within subgroups defined by combination of PD-L1/ctDNA at C1D1

Model	DFS HR (95% CI)	OS HR (95% CI)	No. of patients
Atezolizumab Arm: PD-L1(+) vs PD-L1(–)			PD-L1(+): 140 PD-L1(–): 160 Total: 300
Univariate*	0.72 (0.52–0.99)	0.65 (0.42–1.01)	
IMvigor010 primary†	0.73 (0.53–1.01)	0.64 (0.42–1.00)	
Multivariate‡	0.76 (0.55–1.04)	0.68 (0.44–1.05)	
Observation Arm: PD-L1(+) vs PD-L1(–)			PD-L1(+): 126 PD-L1(–): 145 Total: 271
Univariate	0.54 (0.38–0.75)	0.59 (0.38–0.93)	
IMvigor010 primary	0.55 (0.39–0.78)	0.59 (0.37–0.93)	
Multivariate	0.56 (0.40–0.80)	0.60 (0.38–0.95)	
PD-L1(+) subgroup: Atezolizumab vs observation			Atezolizumab: 140 Observation: 136 Total: 276
Univariate	1.09 (0.76–1.56)	0.99 (0.61–1.60)	
IMvigor010 primary	1.05 (0.73–1.51)	0.92 (0.57–1.50)	
Multivariate	1.06 (0.74–1.52)	0.95 (0.59–1.55)	
PD-L1(–) subgroup: Atezolizumab vs observation			Atezolizumab: 160 Observation: 145 Total: 305
Univariate	0.79 (0.59–1.07)	0.87 (0.59–1.28)	
IMvigor010 primary	0.78 (0.58–1.05)	0.87 (0.59–1.29)	
Multivariate	0.79 (0.59–1.06)	0.87 (0.59–1.29)	
C1D1 ctDNA(+)/PD-L1 (+) subgroup: Atezolizumab vs observation			Atezolizumab: 62 Observation: 40 Total: 102
Univariate	0.52 (0.33–0.82)	0.46 (0.26–0.82)	
IMvigor010 primary	0.50 (0.31–0.80)	0.45 (0.25–0.80)	
Multivariate	0.49 (0.30–0.78)	0.45 (0.25–0.79)	
C1D1 ctDNA(+)/PD-L1 (–) subgroup: Atezolizumab vs observation			Atezolizumab: 54 Observation: 58 Total: 112
Univariate	0.70 (0.46–1.06)	0.79 (0.48–1.3)	
IMvigor010 primary	0.64 (0.42–0.98)	0.71 (0.42–1.18)	
Multivariate	0.63 (0.41–0.97)	0.75 (0.45–1.25)	
C1D1 ctDNA(–)/PD-L1 (+) subgroup: Atezolizumab vs observation			Atezolizumab: 78 Observation: 96 Total: 174
Univariate	1.23 (0.67–2.26)	1.38 (0.53–3.57)	
IMvigor010 primary	1.35 (0.73–2.49)	1.44 (0.55–3.80)	
Multivariate	1.33 (0.72–2.45)	1.51 (0.58–3.96)	
C1D1 ctDNA(–)/PD-L1(–) subgroup: Atezolizumab vs observation			Atezolizumab: 106 Observation: 87 Total: 193
Univariate	0.96 (0.63–1.48)	1.10 (0.58–2.09)	
IMvigor010 primary	0.96 (0.62–1.47)	1.13 (0.59–2.16)	
Multivariate	0.98 (0.64–1.50)	1.11 (0.58–2.11)	

* Univariate Cox proportional-hazard model was prespecified in ctDNA statistical analysis plan. † Stratified Cox proportional-hazards model was used for IMvigor010 primary analysis. Stratification factors were: nodal status (+ or –) and tumour stage (≤ pT2 or pT3/4); in this subgroup analysis defined by PD-L1 status, PD-L1 status was not included as a stratification factor. ‡ Multivariable Cox proportional-hazards regression analysis was prespecified in ctDNA statistical analysis plan. Stratification factors were: nodal status (+ or –), tumour stage (≤ pT2 or pT3/4), prior neoadjuvant chemotherapy (yes or no), and number of lymph nodes (<10 or ≥10); in this subgroup analysis defined by PD-L1 status, PD-L1 status was not included as a stratification factor.

Figure 1

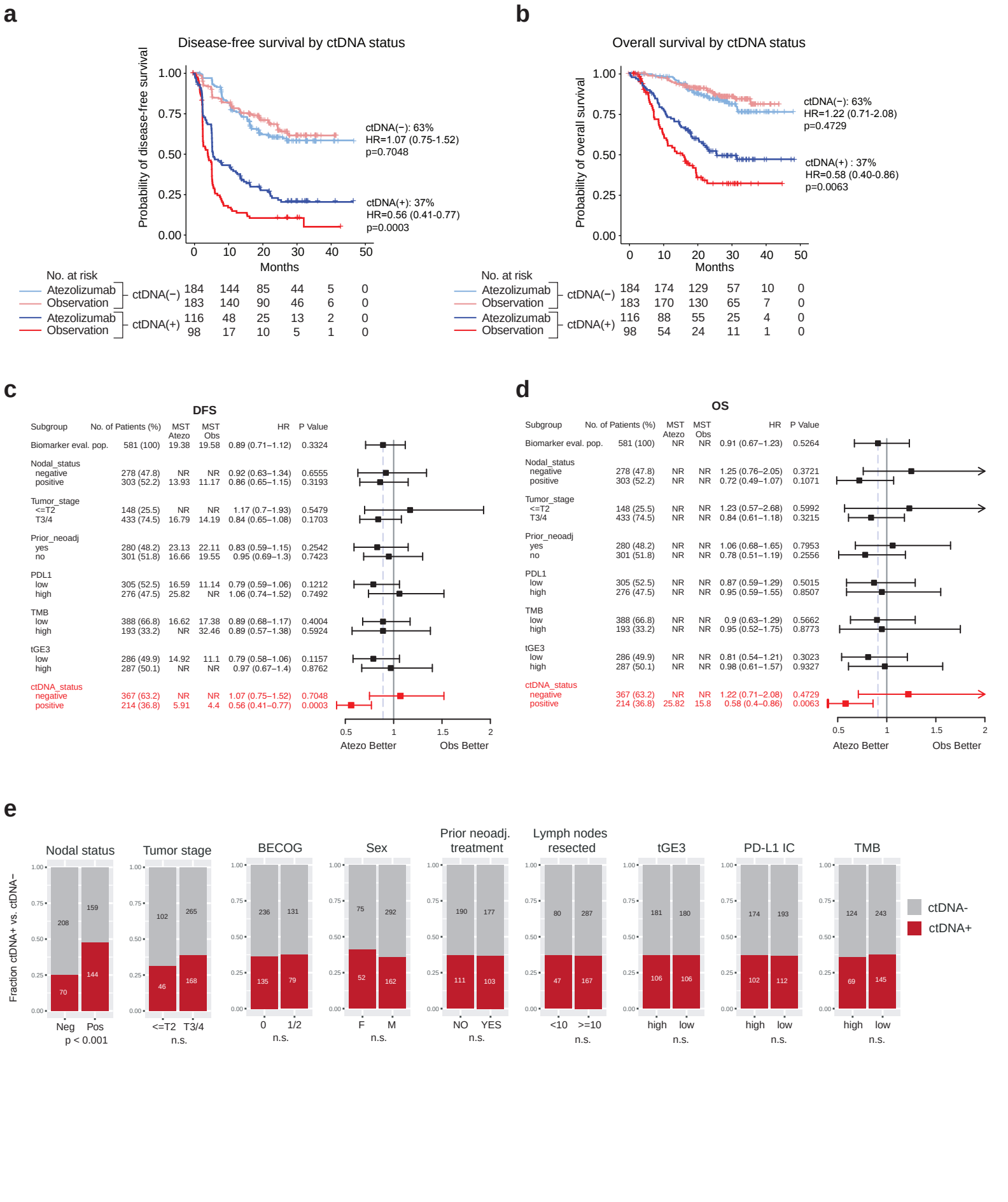
a
Disease-free survival by ctDNA status
Probability of disease-free survival
1.00
0.75
0.50
0.25
0.00
0
10
20
30
40
50
Months
ctDNA(−): 63%
HR=1.07 (0.75-1.52)
p=0.7048
ctDNA(+): 37%
HR=0.56 (0.41-0.77)
p=0.0003
No. at risk
Atezolizumab
Observation
ctDNA(−)
184 144 85 44 5 0
183 140 90 46 6 0
Atezolizumab
Observation
ctDNA(+)
116 48 25 13 2 0
98 17 10 5 1 0
b
Overall survival by ctDNA status
Probability of overall survival
1.00
0.75
0.50
0.25
0.00
0
10
20
30
40
50
Months
ctDNA(−): 63%
HR=1.22 (0.71-2.08)
p=0.4729
ctDNA(+) : 37%
HR=0.58 (0.40-0.86)
p=0.0063
No. at risk
Atezolizumab
Observation
ctDNA(−)
184 174 129 57 10 0
183 170 130 65 7 0
Atezolizumab
Observation
ctDNA(+)
116 88 55 25 4 0
98 54 24 11 1 0
c
DFS
Subgroup
No. of Patients (%)
MST Atezo
MST Obs
HR
P Value
Biomarker eval. pop. 581 (100) 19.38 19.58 0.89 (0.71–1.12) 0.3324
Nodal_status
negative 278 (47.8) NR NR 0.92 (0.63–1.34) 0.6555
positive 303 (52.2) 13.93 11.17 0.86 (0.65–1.15) 0.3193
Tumor_stage
<=T2 148 (25.5) NR NR 1.17 (0.7–1.93) 0.5479
T3/4 433 (74.5) 16.79 14.19 0.84 (0.65–1.08) 0.1703
Prior_neoadj
yes 280 (48.2) 23.13 22.11 0.83 (0.59–1.15) 0.2542
no 301 (51.8) 16.66 19.55 0.95 (0.69–1.3) 0.7423
PDL1
low 305 (52.5) 16.59 11.14 0.79 (0.59–1.06) 0.1212
high 276 (47.5) 25.82 NR 1.06 (0.74–1.52) 0.7492
TMB
low 388 (66.8) 16.62 17.38 0.89 (0.68–1.17) 0.4004
high 193 (33.2) NR 32.46 0.89 (0.57–1.38) 0.5924
tGE3
low 286 (49.9) 14.92 11.1 0.79 (0.58–1.06) 0.1157
high 287 (50.1) NR NR 0.97 (0.67–1.4) 0.8762
ctDNA_status
negative 367 (63.2) NR NR 1.07 (0.75–1.52) 0.7048
positive 214 (36.8) 5.91 4.4 0.56 (0.41–0.77) 0.0003
0.5
1
1.5
2
Atezo Better
Obs Better
d
OS
Subgroup
No. of Patients (%)
MST Atezo
MST Obs
HR
P Value
Biomarker eval. pop. 581 (100) NR NR 0.91 (0.67–1.23) 0.5264
Nodal_status
negative 278 (47.8) NR NR 1.25 (0.76–2.05) 0.3721
positive 303 (52.2) NR NR 0.72 (0.49–1.07) 0.1071
Tumor_stage
<=T2 148 (25.5) NR NR 1.23 (0.57–2.68) 0.5992
T3/4 433 (74.5) NR NR 0.84 (0.61–1.18) 0.3215
Prior_neoadj
yes 280 (48.2) NR NR 1.06 (0.68–1.65) 0.7953
no 301 (51.8) NR NR 0.78 (0.51–1.19) 0.2556
PDL1
low 305 (52.5) NR NR 0.87 (0.59–1.29) 0.5015
high 276 (47.5) NR NR 0.95 (0.59–1.55) 0.8507
TMB
low 388 (66.8) NR NR 0.9 (0.63–1.29) 0.5662
high 193 (33.2) NR NR 0.95 (0.52–1.75) 0.8773
tGE3
low 286 (49.9) NR NR 0.81 (0.54–1.21) 0.3023
high 287 (50.1) NR NR 0.98 (0.61–1.57) 0.9327
ctDNA_status
negative 367 (63.2) NR NR 1.22 (0.71–2.08) 0.4729
positive 214 (36.8) 25.82 15.8 0.58 (0.4–0.86) 0.0063
0.5
1
1.5
2
Atezo Better
Obs Better
e
Nodal status
Tumor stage
BECOG
Sex
Prior neoadj. treatment
Lymph nodes resected
tGE3
PD-L1 IC
TMB
Fraction ctDNA+ vs. ctDNA−
1.00
0.75
0.50
0.25
0.00
208 159 70 144
Neg Pos
p < 0.001
102 265 46 168
<=T2 T3/4
n.s.
236 131 135 79
0 1/2
n.s.
75 292 52 162
F M
n.s.
190 177 111 103
NO YES
n.s.
80 287 47 167
<10 >=10
n.s.
181 180 106 106
high low
n.s.
174 193 102 112
high low
n.s.
124 243 69 145
high low
n.s.
ctDNA-
ctDNA+

Figure 2

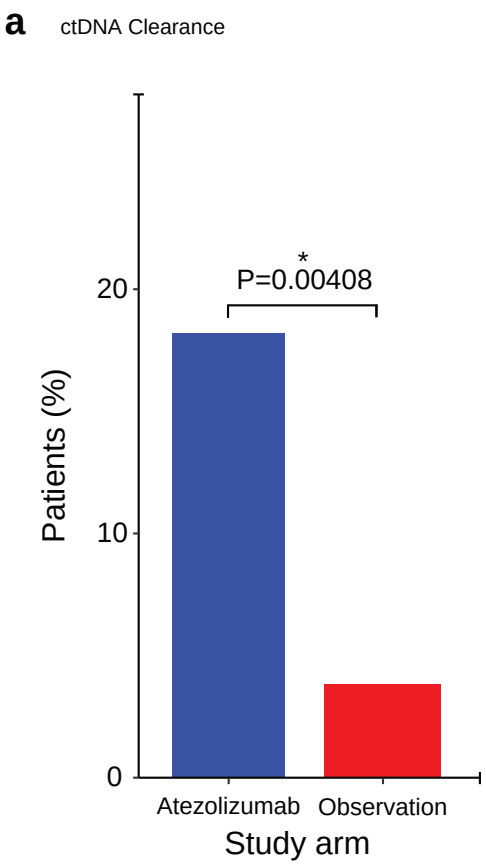

cDNA(+) patients at C1D1	n=99	n=79
Pos > Pos	81 (81.82%)	76 (96.2%)
Pos > Neg	18 (18.8%)	3 (3.8%)

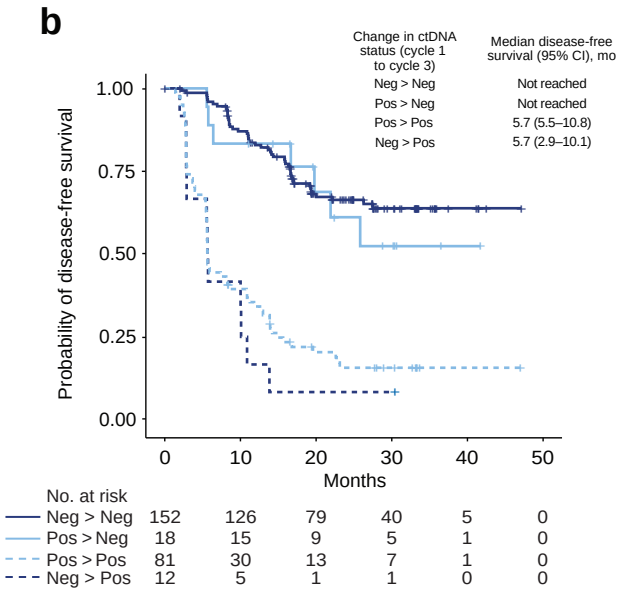

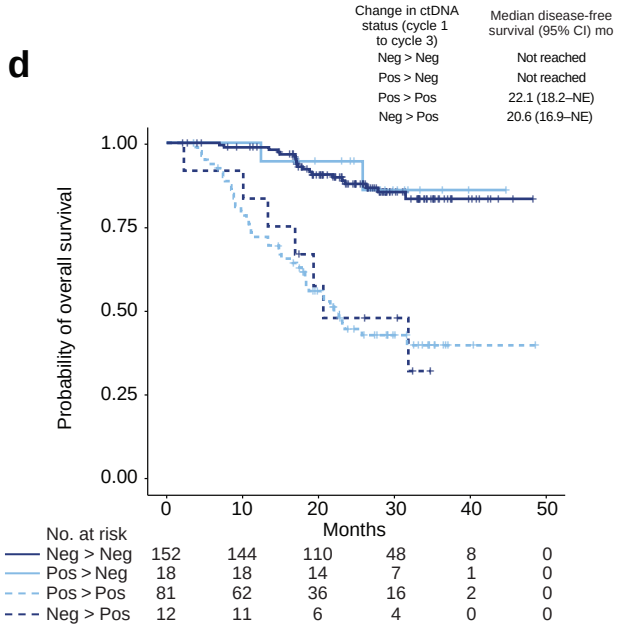

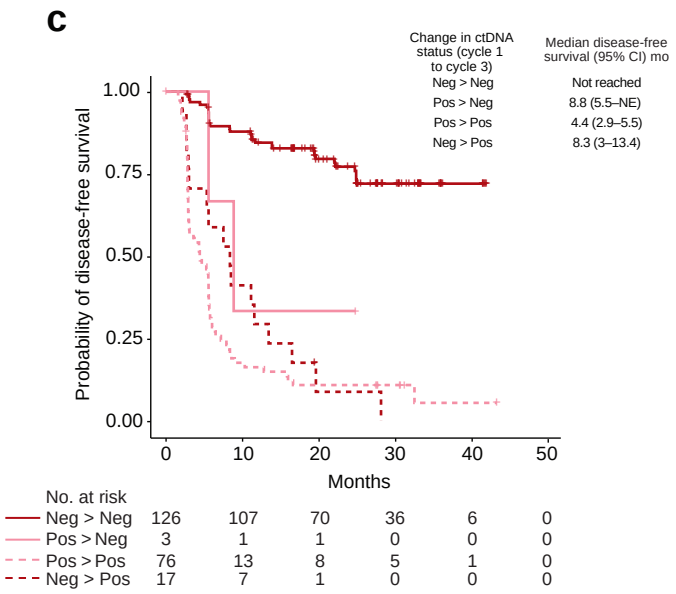

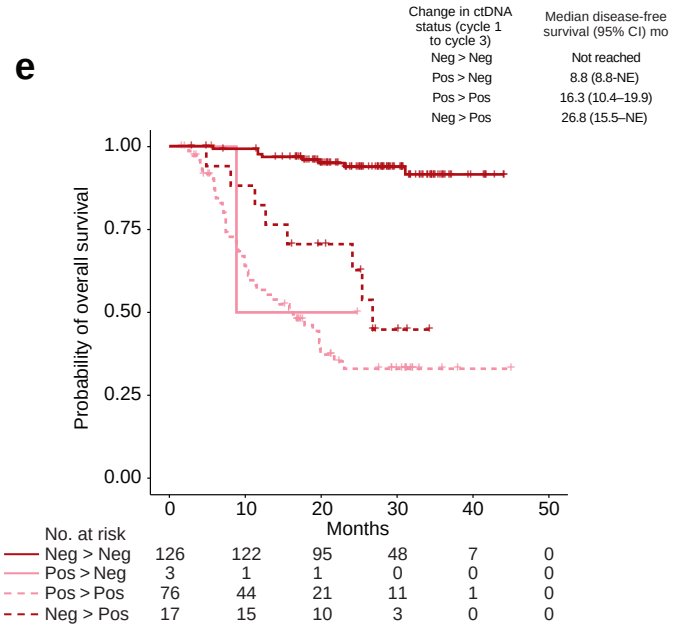

Figure 3

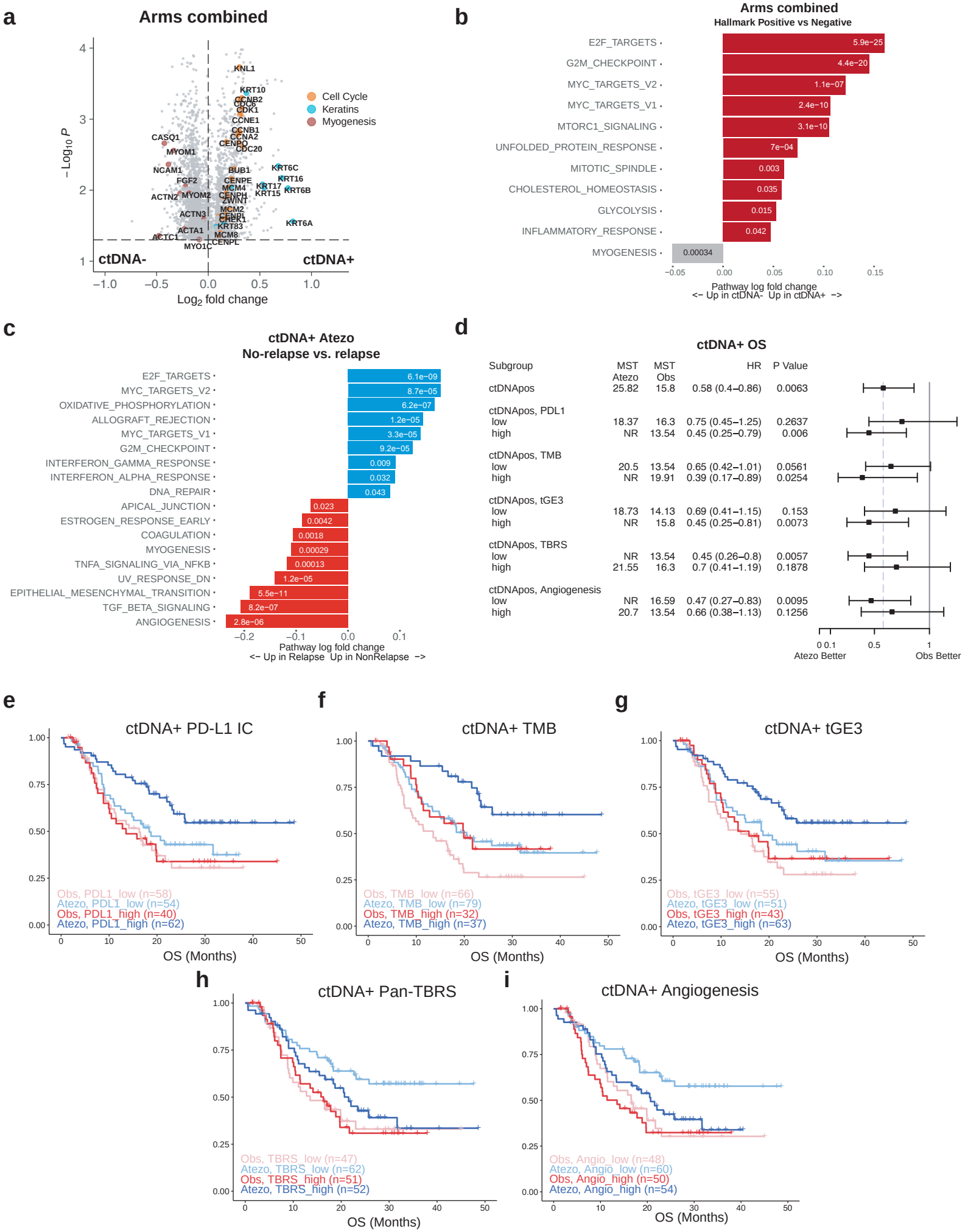
a
Arms combined
Cell Cycle
Keratins
Myogenesis
KNL1
KRT10
CCNB2
CDC6
CDK1
CCNE1
CCNB1
CCNA2
CENPO
CDC20
CASQ1
MYOM1
NCAM1
FGF2
ACTN2
MYOM2
ACTN3
ACTA1
ACTC1
MYO1C
BUB1
CENPE
MCM4
CENPH
ZWINT
MCM2
CENPI
CHEK1
KRT83
MCM8
CENPL
KRT6C
KRT16
KRT17
KRT15
KRT6B
KRT6A
ctDNA-
ctDNA+
−Log10 P
Log2 fold change
b
Arms combined
Hallmark Positive vs Negative
E2F_TARGETS
G2M_CHECKPOINT
MYC_TARGETS_V2
MYC_TARGETS_V1
MTORC1_SIGNALING
UNFOLDED_PROTEIN_RESPONSE
MITOTIC_SPINDLE
CHOLESTEROL_HOMEOSTASIS
GLYCOLYSIS
INFLAMMATORY_RESPONSE
MYOGENESIS
5.9e−25
4.4e−20
1.1e−07
2.4e−10
3.1e−10
7e−04
0.003
0.035
0.015
0.042
0.00034
Pathway log fold change
<− Up in ctDNA- Up in ctDNA+ −>
c
ctDNA+ Atezo
No-relapse vs. relapse
E2F_TARGETS
MYC_TARGETS_V2
OXIDATIVE_PHOSPHORYLATION
ALLOGRAFT_REJECTION
MYC_TARGETS_V1
G2M_CHECKPOINT
INTERFERON_GAMMA_RESPONSE
INTERFERON_ALPHA_RESPONSE
DNA_REPAIR
APICAL_JUNCTION
ESTROGEN_RESPONSE_EARLY
COAGULATION
MYOGENESIS
TNFA_SIGNALING_VIA_NFKB
UV_RESPONSE_DN
EPITHELIAL_MESENCHYMAL_TRANSITION
TGF_BETA_SIGNALING
ANGIOGENESIS
6.1e−09
8.7e−05
6.2e−07
1.2e−05
3.3e−05
9.2e−05
0.009
0.032
0.043
0.023
0.0042
0.0018
0.00029
0.00013
1.2e−05
5.5e−11
8.2e−07
2.8e−06
Pathway log fold change
<− Up in Relapse Up in NonRelapse −>
d
ctDNA+ OS
Subgroup
MST Atezo
MST Obs
HR
P Value
ctDNApos 25.82 15.8 0.58 (0.4–0.86) 0.0063
ctDNApos, PDL1
low 18.37 16.3 0.75 (0.45–1.25) 0.2637
high NR 13.54 0.45 (0.25–0.79) 0.006
ctDNApos, TMB
low 20.5 13.54 0.65 (0.42–1.01) 0.0561
high NR 19.91 0.39 (0.17–0.89) 0.0254
ctDNApos, tGE3
low 18.73 14.13 0.69 (0.41–1.15) 0.153
high NR 15.8 0.45 (0.25–0.81) 0.0073
ctDNApos, TBRS
low NR 13.54 0.45 (0.26–0.8) 0.0057
high 21.55 16.3 0.7 (0.41–1.19) 0.1878
ctDNApos, Angiogenesis
low NR 16.59 0.47 (0.27–0.83) 0.0095
high 20.7 13.54 0.66 (0.38–1.13) 0.1256
Atezo Better
Obs Better
e
ctDNA+ PD-L1 IC
Obs, PDL1_low (n=58)
Atezo, PDL1_low (n=54)
Obs, PDL1_high (n=40)
Atezo, PDL1_high (n=62)
OS (Months)
f
ctDNA+ TMB
Obs, TMB_low (n=66)
Atezo, TMB_low (n=79)
Obs, TMB_high (n=32)
Atezo, TMB_high (n=37)
OS (Months)
g
ctDNA+ tGE3
Obs, tGE3_low (n=55)
Atezo, tGE3_low (n=51)
Obs, tGE3_high (n=43)
Atezo, tGE3_high (n=63)
OS (Months)
h
ctDNA+ Pan-TBRS
Obs, TBRS_low (n=47)
Atezo, TBRS_low (n=62)
Obs, TBRS_high (n=51)
Atezo, TBRS_high (n=52)
OS (Months)
i
ctDNA+ Angiogenesis
Obs, Angio_low (n=48)
Atezo, Angio_low (n=60)
Obs, Angio_high (n=50)
Atezo, Angio_high (n=54)
OS (Months)

Figure 4

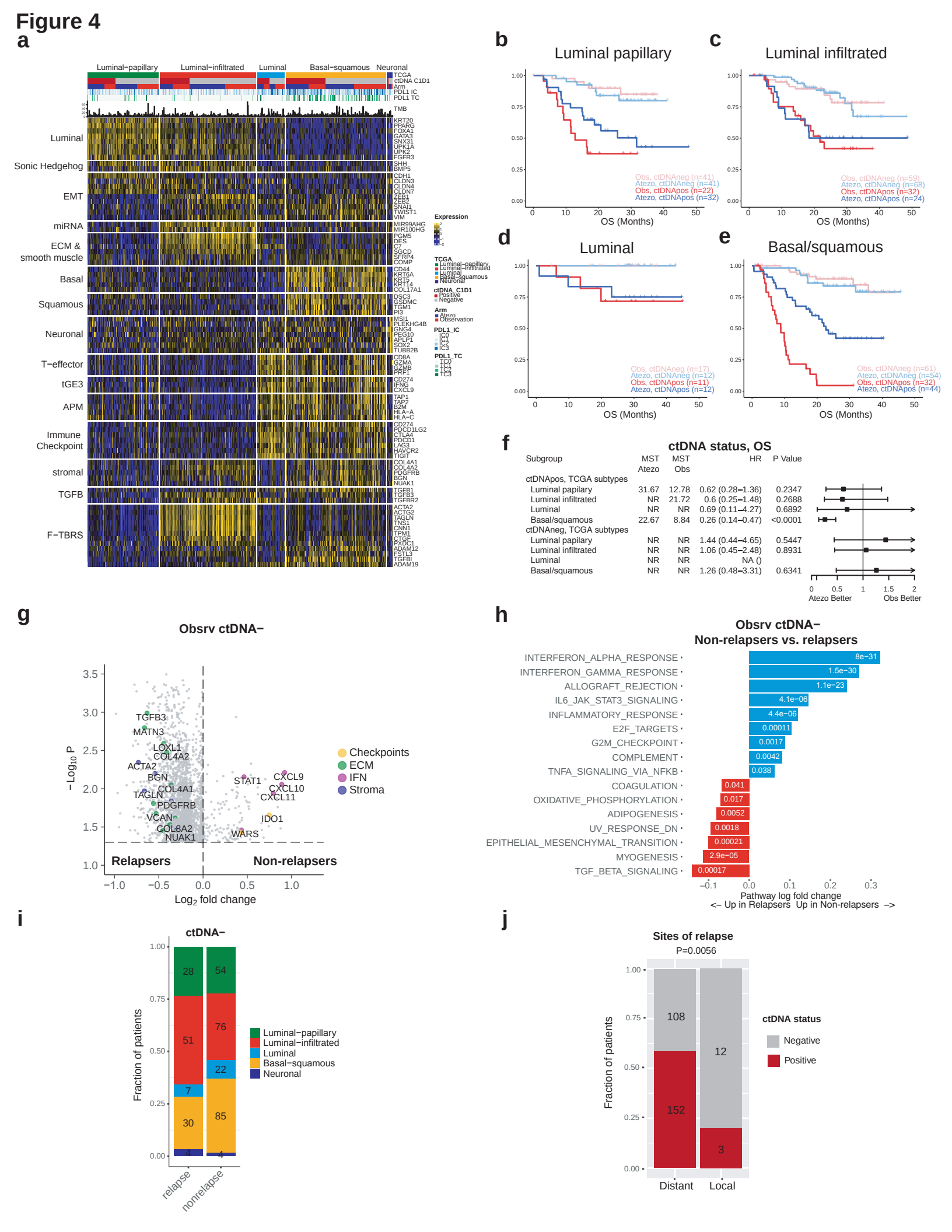
a
Luminal−papillary
Luminal−infiltrated
Luminal
Basal−squamous
Neuronal
TCGA
ctDNA C1D1
Arm
PDL1 IC
PDL1 TC
TMB
Luminal
Sonic Hedgehog
EMT
miRNA
ECM & smooth muscle
Basal
Squamous
Neuronal
T−effector
tGE3
APM
Immune Checkpoint
stromal
TGFB
F−TBRS
Expression
b
Luminal papillary
Obs, ctDNAneg (n=41)
Atezo, ctDNAneg (n=41)
Obs, ctDNApos (n=22)
Atezo, ctDNApos (n=32)
OS (Months)
c
Luminal infiltrated
Obs, ctDNAneg (n=59)
Atezo, ctDNAneg (n=68)
Obs, ctDNApos (n=32)
Atezo, ctDNApos (n=24)
OS (Months)
d
Luminal
Obs, ctDNAneg (n=17)
Atezo, ctDNAneg (n=12)
Obs, ctDNApos (n=11)
Atezo, ctDNApos (n=12)
OS (Months)
e
Basal/squamous
Obs, ctDNAneg (n=61)
Atezo, ctDNAneg (n=54)
Obs, ctDNApos (n=32)
Atezo, ctDNApos (n=44)
OS (Months)
f
ctDNA status, OS
Subgroup | MST Atezo | MST Obs | HR | P Value
ctDNApos, TCGA subtypes
Luminal papilary | 31.67 | 12.78 | 0.62 (0.28–1.36) | 0.2347
Luminal infiltrated | NR | 21.72 | 0.6 (0.25–1.48) | 0.2688
Luminal | NR | NR | 0.69 (0.11–4.27) | 0.6892
Basal/squamous | 22.67 | 8.84 | 0.26 (0.14–0.47) | <0.0001
ctDNAneg, TCGA subtypes
Luminal papilary | NR | NR | 1.44 (0.44–4.65) | 0.5447
Luminal infiltrated | NR | NR | 1.06 (0.45–2.48) | 0.8931
Luminal | NR | NR | NA () |
Basal/squamous | NR | NR | 1.26 (0.48–3.31) | 0.6341
Atezo Better
Obs Better
g
Obsrv ctDNA−
−Log10 P
Log2 fold change
Relapsers
Non-relapsers
Checkpoints
ECM
IFN
Stroma
TGFB3
MATN3
LOXL1
COL4A2
ACTA2
BGN
COL4A1
TAGLN
PDGFRB
VCAN
COL8A2
NUAK1
STAT1
CXCL9
CXCL10
CXCL11
IDO1
WARS
h
Obsrv ctDNA−
Non-relapsers vs. relapsers
INTERFERON_ALPHA_RESPONSE
INTERFERON_GAMMA_RESPONSE
ALLOGRAFT_REJECTION
IL6_JAK_STAT3_SIGNALING
INFLAMMATORY_RESPONSE
E2F_TARGETS
G2M_CHECKPOINT
COMPLEMENT
TNFA_SIGNALING_VIA_NFKB
COAGULATION
OXIDATIVE_PHOSPHORYLATION
ADIPOGENESIS
UV_RESPONSE_DN
EPITHELIAL_MESENCHYMAL_TRANSITION
MYOGENESIS
TGF_BETA_SIGNALING
8e−31
1.5e−30
1.1e−23
4.1e−06
4.4e−06
0.00011
0.0017
0.0042
0.038
0.041
0.017
0.0052
0.0018
0.00021
2.9e−05
0.00017
Pathway log fold change
<– Up in Relapsers Up in Non-relapsers –>
i
ctDNA−
Fraction of patients
relapse
nonrelapse
Luminal−papillary
Luminal−infiltrated
Luminal
Basal−squamous
Neuronal
28
51
7
30
4
54
76
22
85
4
j
Sites of relapse
P=0.0056
Fraction of patients
Distant
Local
ctDNA status
Negative
Positive
108
152
12
3

Figure ED1

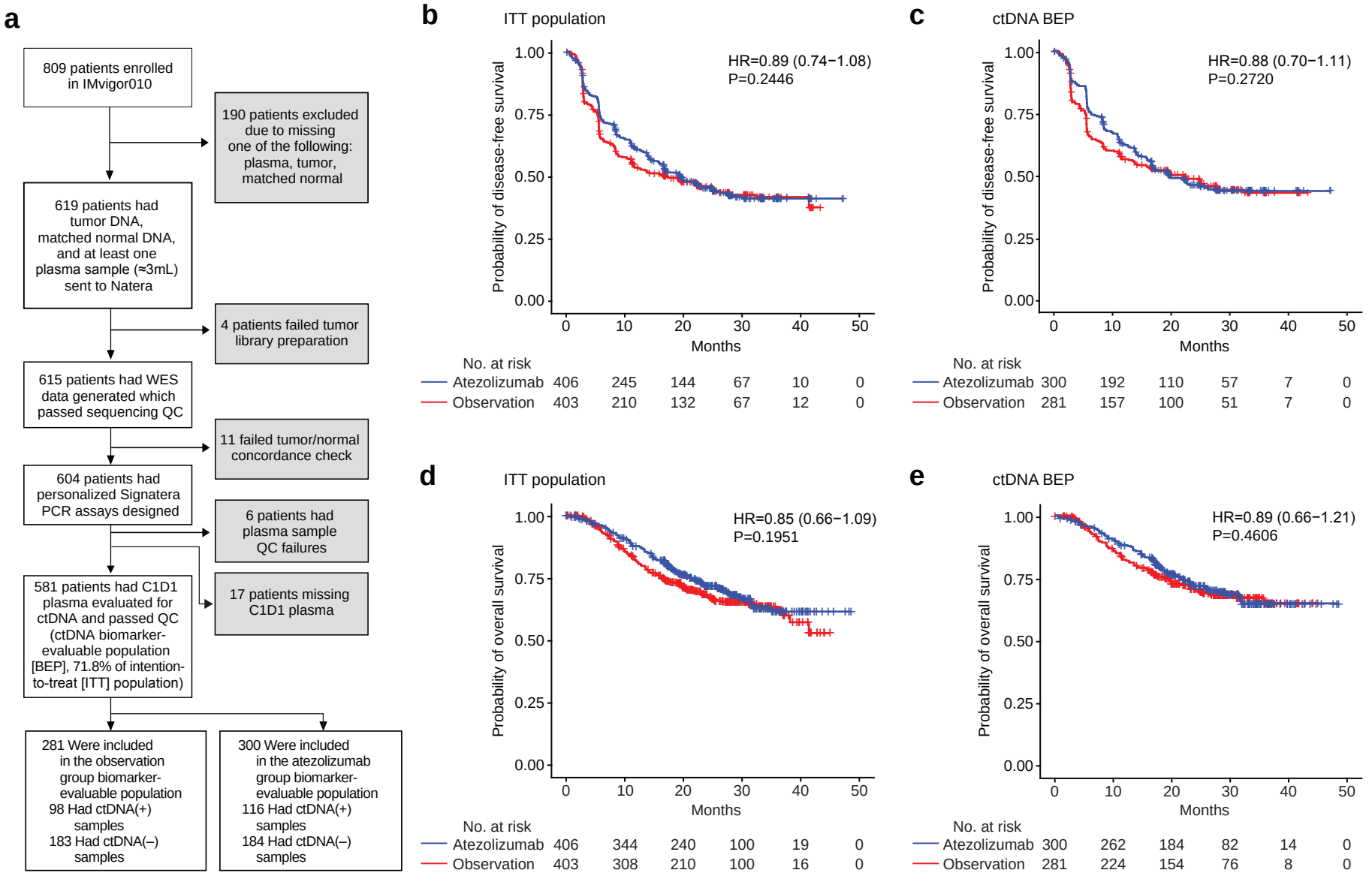
a
809 patients enrolled in IMvigor010
190 patients excluded due to missing one of the following: plasma, tumor, matched normal
619 patients had tumor DNA, matched normal DNA, and at least one plasma sample (≈3mL) sent to Natera
4 patients failed tumor library preparation
615 patients had WES data generated which passed sequencing QC
11 failed tumor/normal concordance check
604 patients had personalized Signatera PCR assays designed
6 patients had plasma sample QC failures
17 patients missing C1D1 plasma
581 patients had C1D1 plasma evaluated for ctDNA and passed QC (ctDNA biomarker-evaluable population [BEP], 71.8% of intention-to-treat [ITT] population)
281 Were included in the observation group biomarker-evaluable population
98 Had ctDNA(+) samples
183 Had ctDNA(–) samples
300 Were included in the atezolizumab group biomarker-evaluable population
116 Had ctDNA(+) samples
184 Had ctDNA(–) samples
b
ITT population
HR=0.89 (0.74−1.08)
P=0.2446
Probability of disease-free survival
Months
No. at risk
Atezolizumab 406 245 144 67 10 0
Observation 403 210 132 67 12 0
c
ctDNA BEP
HR=0.88 (0.70−1.11)
P=0.2720
Probability of disease-free survival
Months
No. at risk
Atezolizumab 300 192 110 57 7 0
Observation 281 157 100 51 7 0
d
ITT population
HR=0.85 (0.66−1.09)
P=0.1951
Probability of overall survival
Months
No. at risk
Atezolizumab 406 344 240 100 19 0
Observation 403 308 210 100 16 0
e
ctDNA BEP
HR=0.89 (0.66−1.21)
P=0.4606
Probability of overall survival
Months
No. at risk
Atezolizumab 300 262 184 82 14 0
Observation 281 224 154 76 8 0

Figure ED2

a Mean MTM vs DFS (C1D1, observation arm)

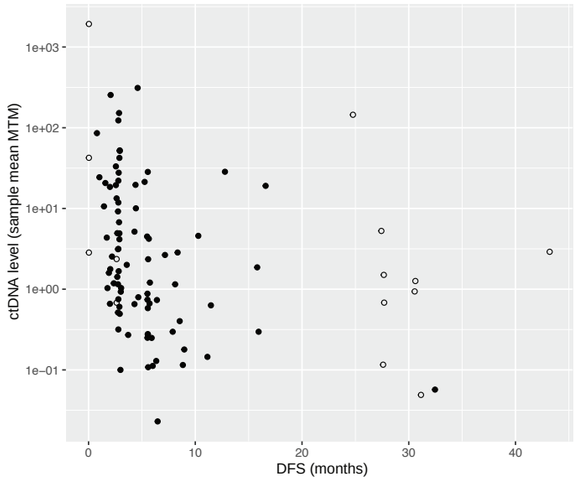

b DFS based on MTM (median split; C1D1, observation arm)

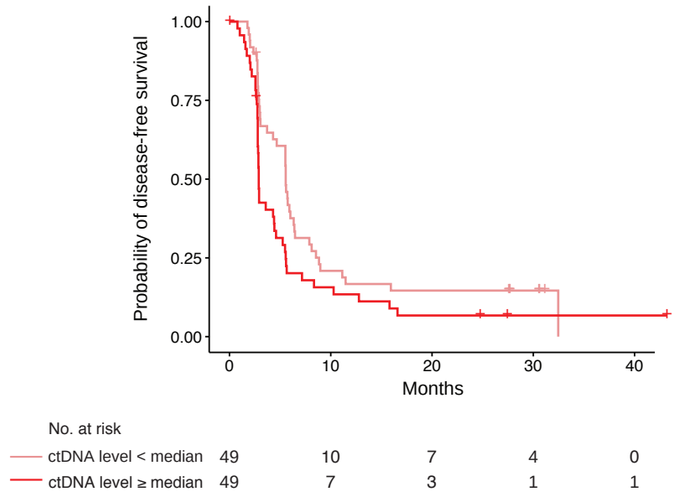

c DFS HRs based on MTM (C1D1, observation arm)

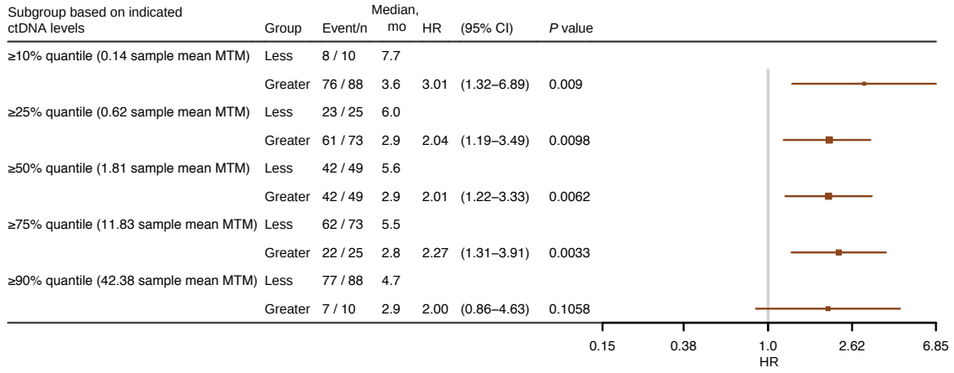

d Mean MTM vs OS (C1D1, observation arm)

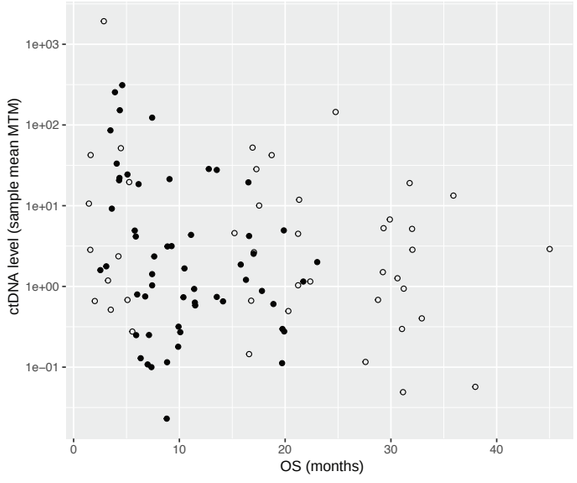

e OS based on MTM (median split; C1D1, observation arm)

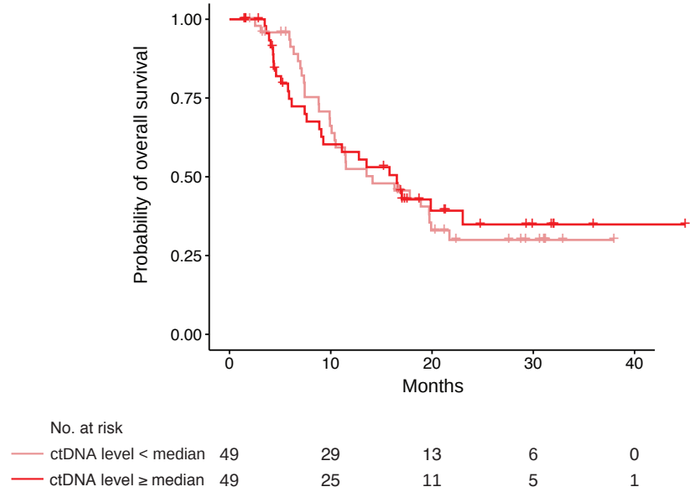

f OS HRs based on MTM (C1D1, observation arm)

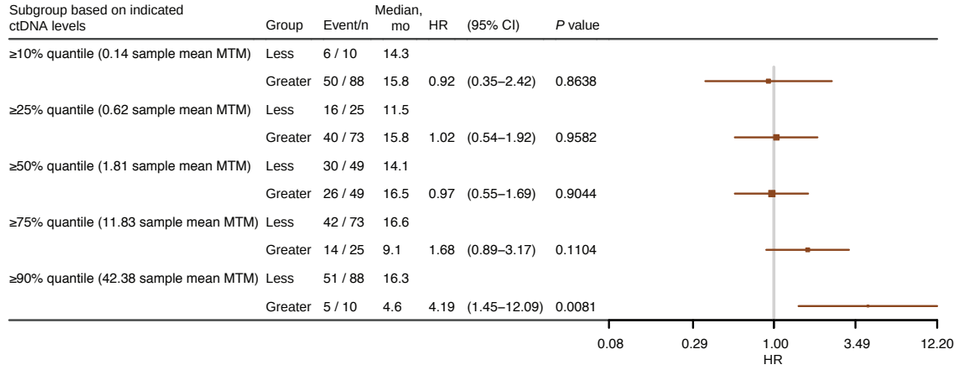

Figure ED3

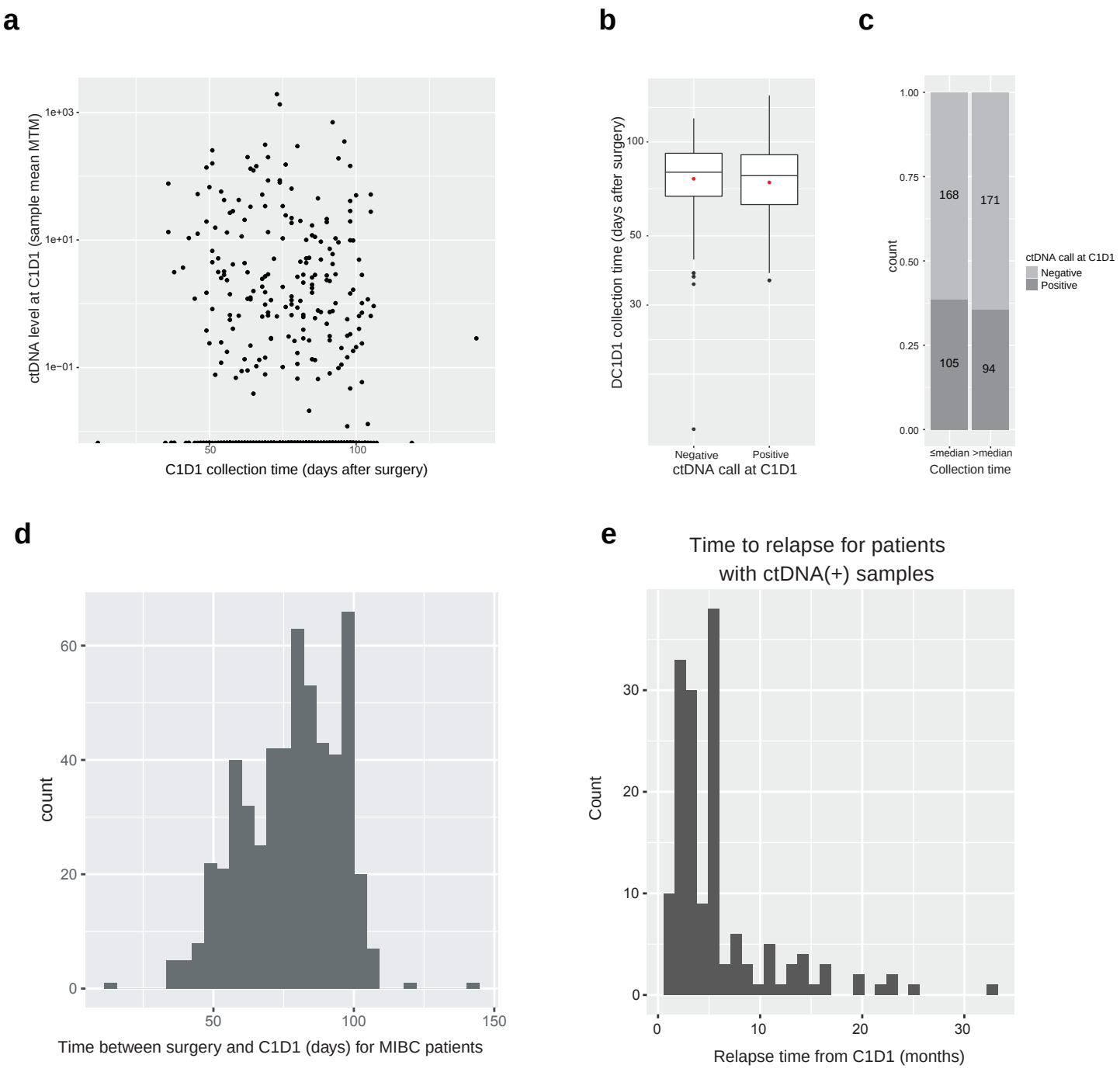
a
ctDNA level at C1D1 (sample mean MTM)
1e+03
1e+01
1e−01
50
100
C1D1 collection time (days after surgery)
b
DC1D1 collection time (days after surgery)
100
50
30
Negative
Positive
ctDNA call at C1D1
c
count
1.00
0.75
0.50
0.25
0.00
168
171
105
94
ctDNA call at C1D1
Negative
Positive
≤median
>median
Collection time
d
count
60
40
20
0
50
100
150
Time between surgery and C1D1 (days) for MIBC patients
e
Time to relapse for patients
with ctDNA(+) samples
Count
30
20
10
0
0
10
20
30
Relapse time from C1D1 (months)

Figure ED4

a ctDNA reduction is higher in the atezo arm than observation arm

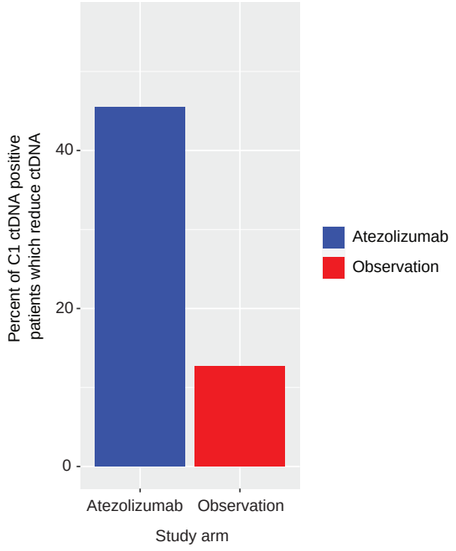

ctDNA(+) patients at C1D1	Atezo	Obs
No reduction	55 (55.6%)	64 (81.0%)
ctDNA reduction	44 (44.4%)	15 (19.0%)

b DFS based on reduction in ctDNA (atezolizumab arm)

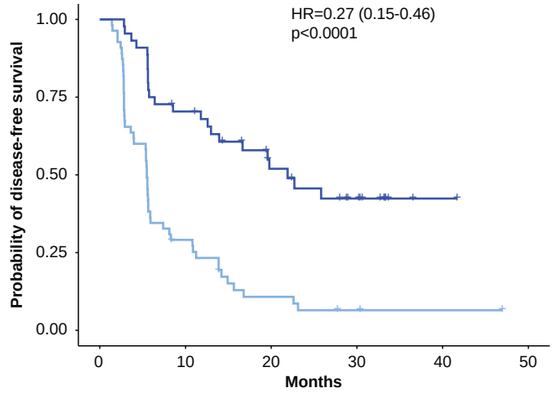

No. at risk						
Reduction in ctDNA (clearance or decrease)	44	30	17	10	1	0
Non-reduction (increase)	55	15	5	2	1	0

c DFS based on reduction in ctDNA (observation arm)

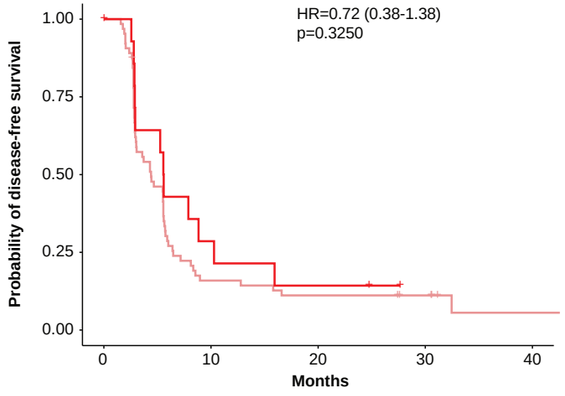

No. at risk						
Reduction in ctDNA (clearance or decrease)	15	4	2	0	0	
Non-reduction (increase)	64	10	7	5	1	

d OS based on reduction in ctDNA (atezolizumab arm)

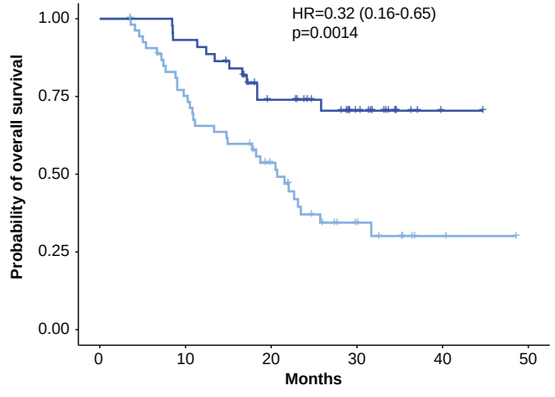

No. at risk						
Reduction in ctDNA (clearance or decrease)	44	41	26	14	1	0
Non-reduction (increase)	55	39	24	9	2	0

e OS based on reduction in ctDNA (observation arm)

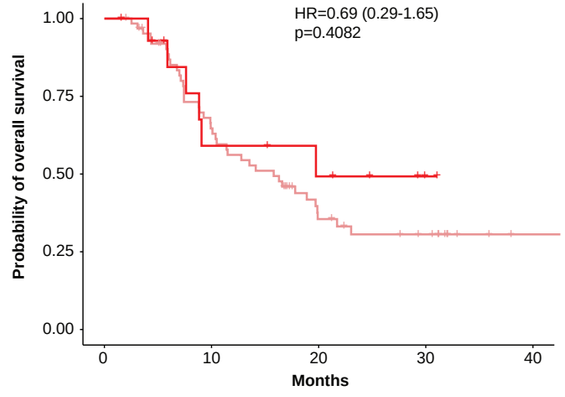

No. at risk						
Reduction in ctDNA (clearance or decrease)	15	7	5	1	0	
Non-reduction (increase)	64	38	17	10	1	

Figure ED5

a DFS based on ctDNA clearance (C1D1+, atezolizumab arm)

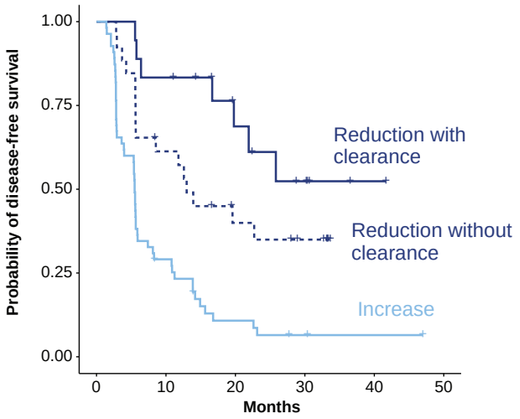

No. at Risk						
Reduction with clearance	18	15	9	5	1	0
Reduction without clearance	26	15	8	5	0	0
Increase	55	15	5	2	1	0

b DFS HRs based on ctDNA reduction thresholds for patients with ctDNA reduction (C1D1 to C3D1, atezolizumab arm)

Subgroup based on indicated ctDNA levels	Group	Event/n	Median, mo	HR	(95% CI)	*P* value
–100% reduction (clearance)	Greater	16 / 26	13.0			
	Less	7 / 18	–	0.58	(0.22–1.52)	0.268
–50% reduction	Greater	8 / 12	12.6			
	Less	15 / 32	25.8	1.05	(0.38–2.89)	0.9235
–25% reduction	Greater	6 / 9	13.9			
	Less	17 / 35	22.7	1.64	(0.54–4.95)	0.3825
–10% reduction	Greater	3 / 4	9.8			
	Less	20 / 40	22.7	0.63	(0.15–2.63)	0.5234

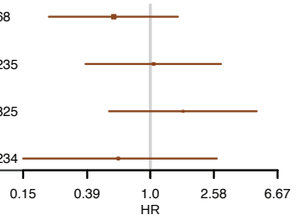

c OS based on ctDNA clearance (C1D1+, atezolizumab arm)

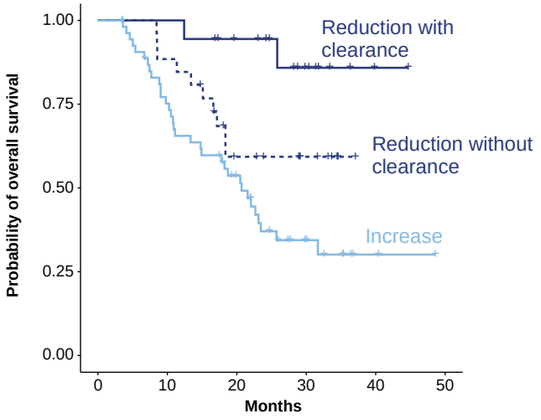

No. at Risk						
Reduction with clearance	18	18	14	7	1	0
Reduction without clearance	26	23	12	7	0	0
Increase	55	39	24	9	2	0

d OS HRs based on ctDNA reduction thresholds for patients with ctDNA reduction (C1D1 to C3D1, atezolizumab arm)

Subgroup based on indicated ctDNA levels	Group	Event/n	Median, mo	HR	(95% CI)	*P* value
–100% reduction (clearance)	Greater	10 / 26	–			
	Less	2 / 18	–	0.23	(0.05–1.13)	0.697
–50% reduction	Greater	4 / 12	–			
	Less	8 / 32	–	1.24	(0.35–4.47)	0.7393
–25% reduction	Greater	2 / 9	–			
	Less	10 / 35	–	2.51	(0.48–13.10)	0.2755
–10% reduction	Greater	1 / 4	–			
	Less	11 / 40	–	1.13	(0.12–10.21)	0.9164

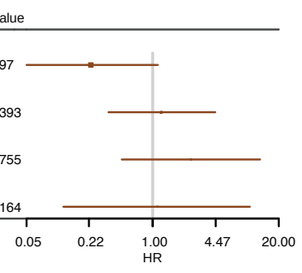

Figure ED6

a

BEP, OS (adjusted for baseline prognostic factors)

Subgroup	No. of Patients (%)	MST Atezo	MST Obs	HR	P Value
BEP	581 (100)	NR	NR	0.91 (0.67–1.23)	0.5264
BEP,nodal_status					
negative	278 (47.8)	NR	NR	1.25 (0.76–2.05)	0.3721
positive	303 (52.2)	NR	NR	0.72 (0.49–1.07)	0.1071
BEP,tumor_stage					
T2_or_less	148 (25.5)	NR	NR	1.23 (0.57–2.68)	0.5992
T3/4	433 (74.5)	NR	NR	0.84 (0.61–1.18)	0.3215
BEP,prior_neoadj					
yes	280 (48.2)	NR	NR	1.06 (0.68–1.65)	0.7953
no	301 (51.8)	NR	NR	0.78 (0.51–1.19)	0.2556
BEP,pdl1_status_IC					
0/1	305 (52.5)	NR	NR	0.87 (0.59–1.29)	0.5015
2/3	276 (47.5)	NR	NR	0.95 (0.59–1.55)	0.8507
BEP,TMB_status					
low	388 (66.8)	NR	NR	0.9 (0.63–1.29)	0.5662
high	193 (33.2)	NR	NR	0.95 (0.52–1.75)	0.8773
BEP,RNA_tGE3_status					
low	286 (49.9)	NR	NR	0.81 (0.54–1.21)	0.3023
high	287 (50.1)	NR	NR	0.98 (0.61–1.57)	0.9327
BEP,RNA_TBRS_status					
low	286 (49.9)	NR	NR	1.01 (0.63–1.63)	0.9552
high	287 (50.1)	NR	NR	0.8 (0.54–1.2)	0.2847
BEP,RNA_Angio_status					
low	281 (49)	NR	NR	0.84 (0.52–1.37)	0.492
high	292 (51)	NR	NR	0.94 (0.63–1.41)	0.7667
BEP,RNA_TCGA					
Lum.Pap.	136 (23.7)	NR	NR	1.09 (0.58–2.06)	0.7902
Lum.Infil.	183 (31.9)	NR	NR	0.83 (0.47–1.47)	0.5235
Lum.	52 (9.1)	NR	NR	1.13 (0.19–6.65)	0.8946
Basal.Squam.	191 (33.3)	NR	NR	0.68 (0.42–1.1)	0.1181
Neuronal	11 (1.9)	17.87	24.11	1204988270.57 (0–Inf)	0.9993

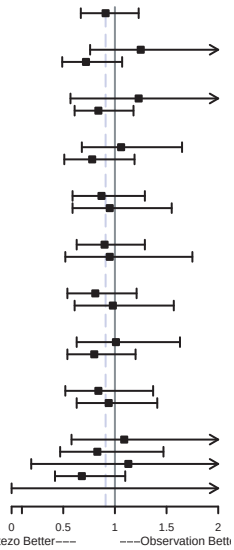

b

ctDNA(–), OS (adjusted for baseline prognostic factors)

Subgroup	No. of Patients (%)	MST Atezo	MST Obs	HR	P Value
ctDNAneg	367 (100)	NR	NR	1.22 (0.71–2.08)	0.4729
ctDNAneg,nodal_status					
negative	208 (56.7)	NR	NR	2.43 (1.07–5.52)	0.033
positive	159 (43.3)	NR	NR	0.62 (0.27–1.41)	0.254
ctDNAneg,tumor_stage					
T2_or_less	102 (27.8)	NR	NR	1.19 (0.38–3.75)	0.7672
T3/4	265 (72.2)	NR	NR	1.17 (0.64–2.16)	0.6113
ctDNAneg,prior_neoadj					
no	190 (51.8)	NR	NR	1.2 (0.58–2.47)	0.6212
yes	177 (48.2)	NR	NR	1.17 (0.52–2.63)	0.7064
ctDNAneg,pdl1_status_IC					
0/1	193 (52.6)	NR	NR	1.11 (0.58–2.11)	0.7577
2/3	174 (47.4)	NR	NR	1.51 (0.58–3.96)	0.3994
ctDNAneg,TMB_status					
high	124 (33.8)	NR	NR	1.73 (0.56–5.36)	0.3408
low	243 (66.2)	NR	NR	1.15 (0.62–2.13)	0.6685
ctDNAneg,RNA_tGE3_status					
high	181 (50.1)	NR	NR	1.36 (0.55–3.34)	0.5004
low	180 (49.9)	NR	NR	1.1 (0.56–2.2)	0.7771
ctDNAneg,RNA_TBRS_status					
high	184 (51)	NR	NR	0.9 (0.47–1.72)	0.7464
low	177 (49)	NR	NR	1.77 (0.67–4.64)	0.247
ctDNAneg,RNA_Angio_status					
high	188 (52.1)	NR	NR	1.32 (0.68–2.56)	0.4168
low	173 (47.9)	NR	NR	0.91 (0.33–2.53)	0.8584
ctDNAneg,RNA_TCGA					
Basal.Squam.	115 (32.6)	NR	NR	1.26 (0.48–3.31)	0.6341
Lum.	29 (8.2)	NR	NR	NA ()	
Lum.Infil.	127 (36)	NR	NR	1.06 (0.45–2.48)	0.8931
Lum.Pap.	82 (23.2)	NR	NR	1.44 (0.44–4.65)	0.5447

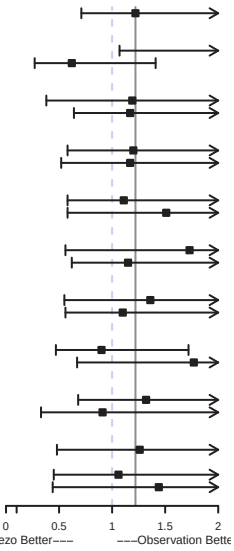

c

ctDNApos, OS (adjusted for baseline prognostic factors)

Subgroup	No. of Patients (%)	MST Atezo	MST Obs	HR	P Value
ctDNApos	214 (100)	25.82	15.8	0.58 (0.4–0.86)	0.0063
ctDNApos,nodal_status					
negative	70 (32.7)	22.05	17.02	0.71 (0.36–1.42)	0.3306
positive	144 (67.3)	25.82	13.54	0.55 (0.34–0.88)	0.0122
ctDNApos,tumor_stage					
T2_or_less	46 (21.5)	NR	NR	1.1 (0.37–3.29)	0.8661
T3/4	168 (78.5)	22.67	11.4	0.53 (0.35–0.81)	0.0031
ctDNApos,prior_neoadj					
yes	103 (48.1)	21.55	17.02	0.88 (0.51–1.54)	0.6625
no	111 (51.9)	NR	11.1	0.4 (0.23–0.68)	0.0008
ctDNApos,pdl1_status_IC					
0/1	112 (52.3)	18.37	16.3	0.75 (0.45–1.25)	0.2637
2/3	102 (47.7)	NR	13.54	0.45 (0.25–0.79)	0.006
ctDNApos,TMB_status					
low	145 (67.8)	20.5	13.54	0.65 (0.42–1.01)	0.0561
high	69 (32.2)	NR	19.91	0.39 (0.17–0.89)	0.0254
ctDNApos,RNA_tGE3_status					
low	106 (50)	18.73	14.13	0.69 (0.41–1.15)	0.153
high	106 (50)	NR	15.8	0.45 (0.25–0.81)	0.0073
ctDNApos,RNA_TBRS_status					
low	109 (51.4)	NR	13.54	0.45 (0.26–0.8)	0.0057
high	103 (48.6)	21.55	16.3	0.7 (0.41–1.19)	0.1878
ctDNApos,RNA_Angio_status					
low	108 (50.9)	NR	16.59	0.47 (0.27–0.83)	0.0095
high	104 (49.1)	20.7	13.54	0.66 (0.38–1.13)	0.1256
ctDNApos,RNA_TCGA					
Lum.Pap.	54 (25.8)	31.67	12.78	0.62 (0.28–1.36)	0.2347
Lum.Infil.	56 (26.8)	NR	21.72	0.6 (0.25–1.48)	0.2688
Lum.	23 (11)	NR	NR	0.69 (0.11–4.27)	0.6892
Basal.Squam.	76 (36.4)	22.67	8.84	0.26 (0.14–0.47)	<0.0001

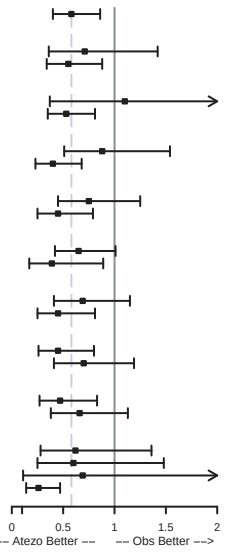

Figure ED7

a

BEP, DFS (adjusted for baseline prognostic factors)

Subgroup	No. of Patients (%)	MST Atezo	MST Obs	HR	P Value
BEP	581 (100)	19.38	19.58	0.89 (0.71–1.12)	0.3324
BEP,nodal_status					
negative	278 (47.8)	NR	NR	0.92 (0.63–1.34)	0.6555
positive	303 (52.2)	13.93	11.17	0.86 (0.65–1.15)	0.3193
BEP,tumor_stage					
T2_or_less	148 (25.5)	NR	NR	1.17 (0.7–1.93)	0.5479
T3/4	433 (74.5)	16.79	14.19	0.84 (0.65–1.08)	0.1703
BEP,prior_neoadj					
yes	280 (48.2)	23.13	22.11	0.83 (0.59–1.15)	0.2542
no	301 (51.8)	16.66	19.55	0.95 (0.69–1.3)	0.7423
BEP,pdl1_status_IC					
0/1	305 (52.5)	16.59	11.14	0.79 (0.59–1.06)	0.1212
2/3	276 (47.5)	25.82	NR	1.06 (0.74–1.52)	0.7492
BEP,TMB_status					
low	388 (66.8)	16.62	17.38	0.89 (0.68–1.17)	0.4004
high	193 (33.2)	NR	32.46	0.89 (0.57–1.38)	0.5924
BEP,RNA_tGE3_status					
low	286 (49.9)	14.92	11.1	0.79 (0.58–1.06)	0.1157
high	287 (50.1)	NR	NR	0.97 (0.67–1.4)	0.8762
BEP,RNA_TBRS_status					
low	286 (49.9)	23.13	NR	1.04 (0.74–1.47)	0.8213
high	287 (50.1)	16.99	11.47	0.77 (0.56–1.05)	0.0943
BEP,RNA_Angio_status					
low	281 (49)	25.82	24.84	0.91 (0.65–1.29)	0.5962
high	292 (51)	16.69	11.17	0.87 (0.64–1.19)	0.3957
BEP,RNA_TCGA					
Lum.Pap.	136 (23.7)	15.87	19.38	1.12 (0.71–1.77)	0.6348
Lum.Infil.	183 (31.9)	22.11	16.46	0.72 (0.48–1.08)	0.1165
Lum.	52 (9.1)	NR	NR	0.71 (0.28–1.79)	0.4631
Basal.Squam.	191 (33.3)	16.99	22.57	0.94 (0.62–1.42)	0.7637
Neuronal	11 (1.9)	5.67	8.33	0.75 (0.08–6.91)	0.8002

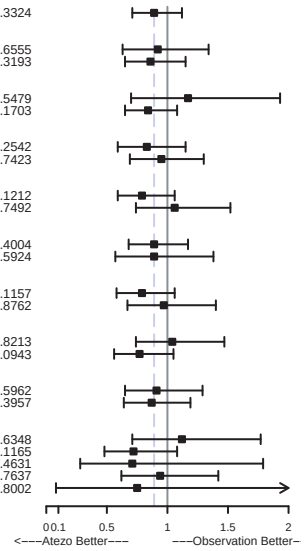

b

ctDNA(–), DFS (adjusted for baseline prognostic factors)

Subgroup	No. of Patients (%)	MST Atezo	MST Obs	HR	P Value
ctDNAneg	367 (100)	NR	NR	1.07 (0.75–1.52)	0.7048
ctDNAneg,nodal_status					
negative	208 (56.7)	NR	NR	1.4 (0.82–2.41)	0.2184
positive	159 (43.3)	NR	28.09	0.85 (0.53–1.37)	0.5069
ctDNAneg,tumor_stage					
T2_or_less	102 (27.8)	NR	NR	1.34 (0.66–2.73)	0.4124
T3/4	265 (72.2)	NR	NR	0.96 (0.64–1.45)	0.8518
ctDNAneg,prior_neoadj					
no	190 (51.8)	NR	NR	1.15 (0.71–1.88)	0.5647
yes	177 (48.2)	NR	NR	0.92 (0.56–1.52)	0.7476
ctDNAneg,pdl1_status_IC					
0/1	193 (52.6)	27.5	28.09	0.98 (0.64–1.5)	0.9147
2/3	174 (47.4)	NR	NR	1.33 (0.72–2.45)	0.3624
ctDNAneg,TMB_status					
high	124 (33.8)	NR	NR	1.36 (0.65–2.87)	0.4131
low	243 (66.2)	NR	NR	0.94 (0.63–1.42)	0.7787
ctDNAneg,RNA_tGE3_status					
high	181 (50.1)	NR	NR	0.91 (0.47–1.73)	0.7624
low	180 (49.9)	19.38	24.87	1.08 (0.7–1.68)	0.7189
ctDNAneg,RNA_TBRS_status					
high	184 (51)	NR	NR	1 (0.63–1.58)	0.9998
low	177 (49)	NR	NR	1.14 (0.64–2.02)	0.6637
ctDNAneg,RNA_Angio_status					
high	188 (52.1)	NR	NR	1.11 (0.7–1.77)	0.6566
low	173 (47.9)	NR	NR	1.01 (0.57–1.79)	0.9785
ctDNAneg,RNA_TCGA					
Basal.Squam.	115 (32.6)	NR	NR	1.33 (0.66–2.67)	0.4316
Lum.	29 (8.2)	NR	NR	0.2 (0.02–2.03)	0.1719
Lum.Infil.	127 (36)	NR	NR	1.12 (0.64–1.95)	0.696
Lum.Pap.	82 (23.2)	27.5	NR	1.47 (0.71–3.04)	0.2963

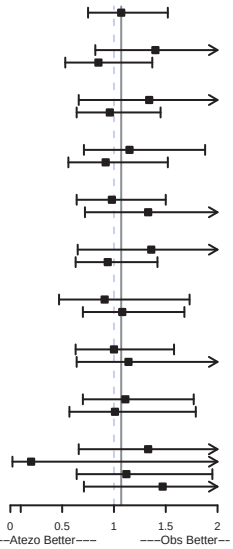

c

ctDNApos, DFS (adjusted for baseline prognostic factors)

Subgroup	No. of Patients (%)	MST Atezo	MST Obs	HR	P Value
ctDNApos	214 (100)	5.91	4.4	0.56 (0.41–0.77)	0.0003
ctDNApos,nodal_status					
negative	70 (32.7)	6.28	3.94	0.49 (0.28–0.86)	0.0135
positive	144 (67.3)	5.91	4.6	0.64 (0.43–0.94)	0.0247
ctDNApos,tumor_stage					
T2_or_less	46 (21.5)	12.98	8.54	0.73 (0.34–1.57)	0.4218
T3/4	168 (78.5)	5.65	3.58	0.52 (0.37–0.74)	0.0003
ctDNApos,prior_neoadj					
yes	103 (48.1)	5.68	4.44	0.67 (0.43–1.06)	0.09
no	111 (51.9)	5.91	3.58	0.45 (0.29–0.7)	0.0004
ctDNApos,pdl1_status_IC					
0/1	112 (52.3)	5.6	4.3	0.63 (0.41–0.97)	0.0343
2/3	102 (47.7)	11.24	4.67	0.49 (0.3–0.78)	0.0027
ctDNApos,TMB_status					
low	145 (67.8)	5.65	4.3	0.72 (0.5–1.05)	0.0886
high	69 (32.2)	16.66	4.6	0.32 (0.16–0.61)	0.0007
ctDNApos,RNA_tGE3_status					
low	106 (50)	5.65	3.02	0.6 (0.39–0.93)	0.0212
high	106 (50)	11.24	5.5	0.5 (0.31–0.8)	0.0037
ctDNApos,RNA_TBRS_status					
low	109 (51.4)	8.11	4.3	0.45 (0.29–0.72)	0.0008
high	103 (48.6)	5.82	4.52	0.58 (0.37–0.91)	0.0181
ctDNApos,RNA_Angio_status					
low	108 (50.9)	12.58	4.4	0.37 (0.23–0.59)	<0.0001
high	104 (49.1)	5.62	4.6	0.72 (0.46–1.14)	0.1602
ctDNApos,RNA_TCGA					
Lum.Pap.	54 (25.8)	5.62	4.3	0.49 (0.26–0.93)	0.029
Lum.Infil.	56 (26.8)	10.56	5.55	0.37 (0.18–0.74)	0.0048
Lum.	23 (11)	22.6	5.49	0.63 (0.19–2.09)	0.4454
Basal.Squam.	76 (36.4)	5.65	4.19	0.46 (0.27–0.78)	0.0039

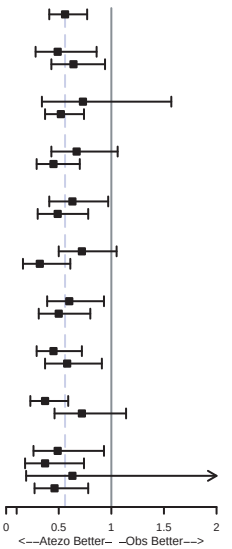

Figure ED8

a

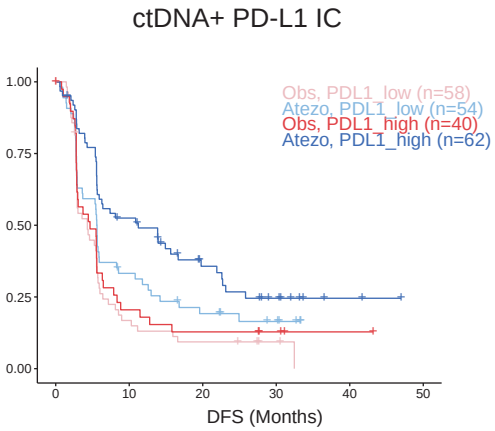

b

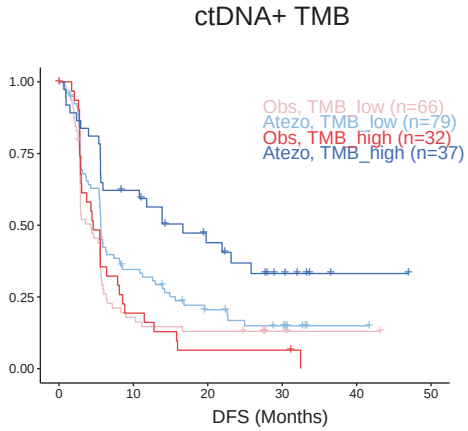

c

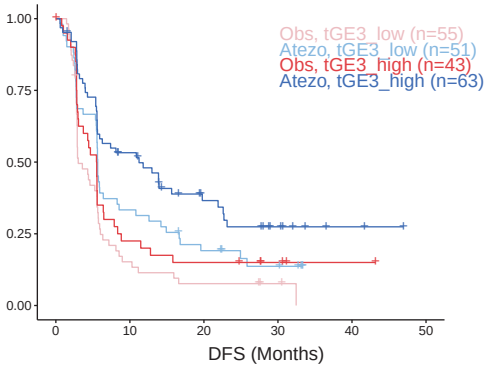

d

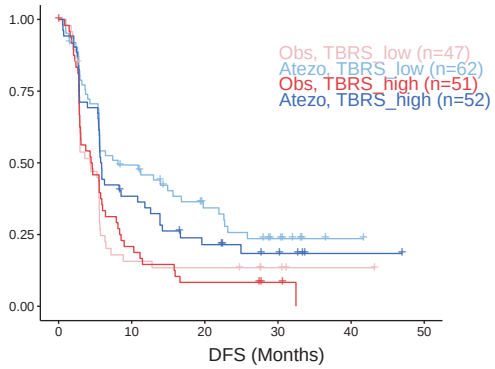

e

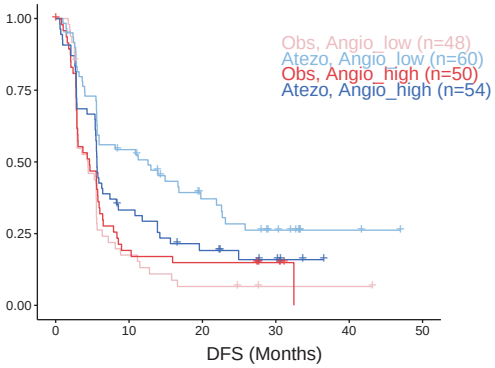

e

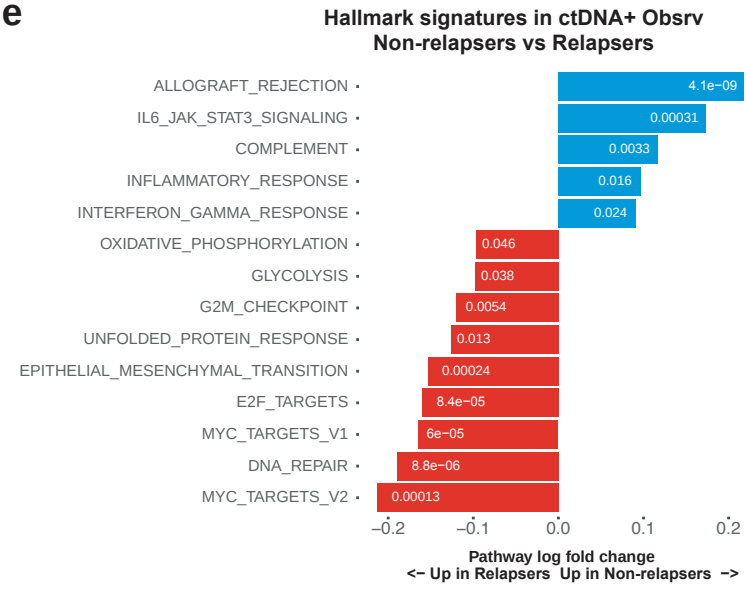

Figure ED9

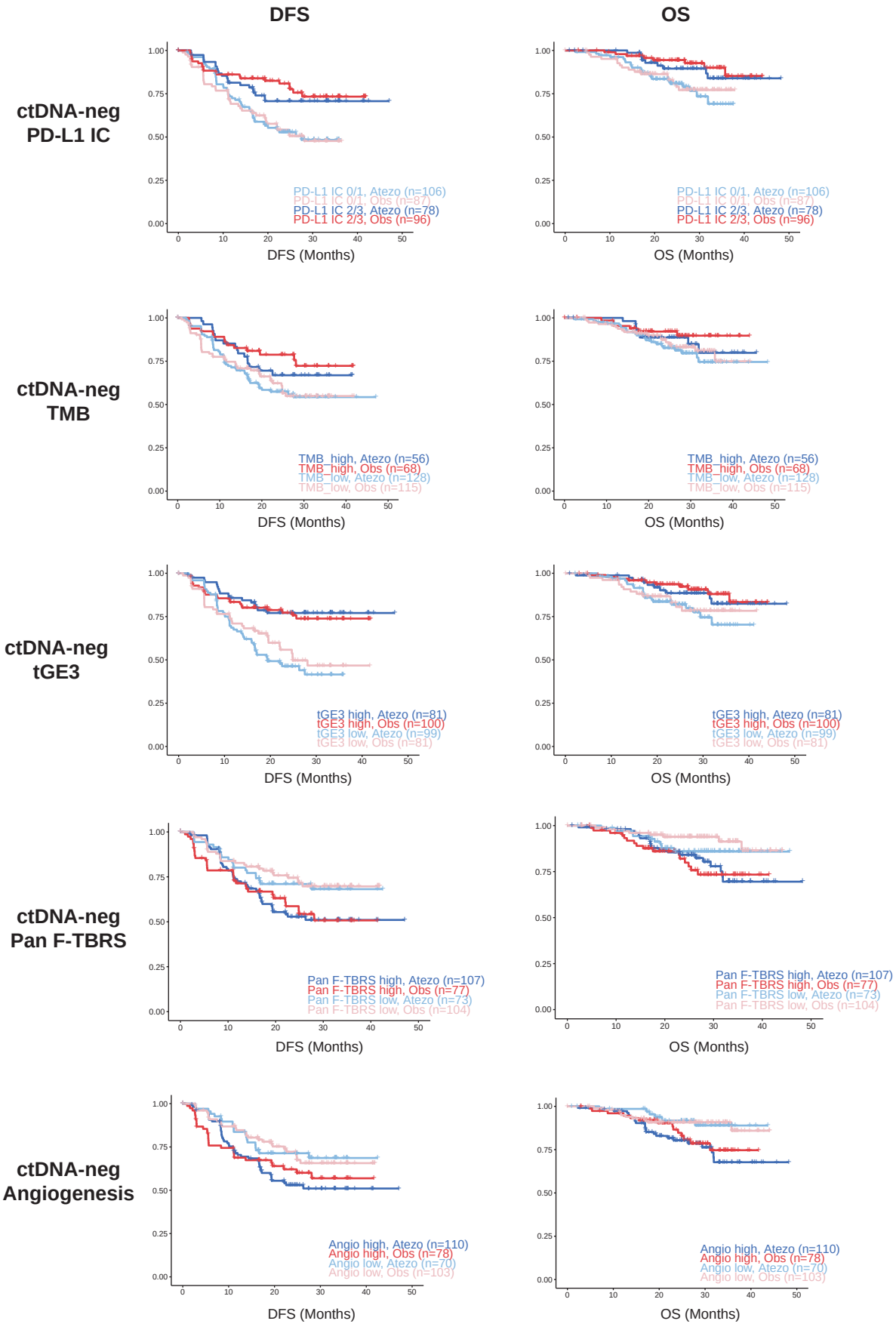
DFS
OS
ctDNA-neg PD-L1 IC
PD-L1 IC 0/1, Atezo (n=106)
PD-L1 IC 0/1, Obs (n=87)
PD-L1 IC 2/3, Atezo (n=78)
PD-L1 IC 2/3, Obs (n=96)
DFS (Months)
OS (Months)
ctDNA-neg TMB
TMB_high, Atezo (n=56)
TMB_high, Obs (n=68)
TMB_low, Atezo (n=128)
TMB_low, Obs (n=115)
ctDNA-neg tGE3
tGE3 high, Atezo (n=81)
tGE3 high, Obs (n=100)
tGE3 low, Atezo (n=99)
tGE3 low, Obs (n=81)
ctDNA-neg Pan F-TBRS
Pan F-TBRS high, Atezo (n=107)
Pan F-TBRS high, Obs (n=77)
Pan F-TBRS low, Atezo (n=73)
Pan F-TBRS low, Obs (n=104)
ctDNA-neg Angiogenesis
Angio high, Atezo (n=110)
Angio high, Obs (n=78)
Angio low, Atezo (n=70)
Angio low, Obs (n=103)

Figure ED10

a DFS in triple-positive patients

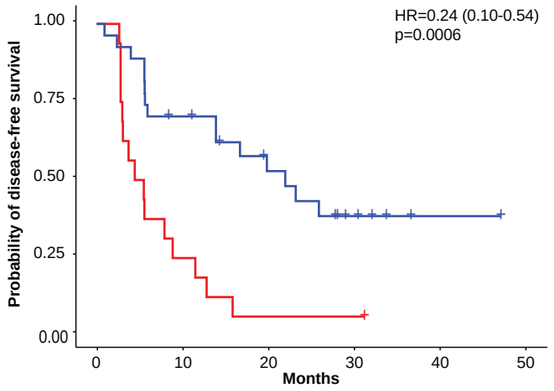

No. at risk						
Atezolizumab	27	18	11	5	1	0
Observation	16	4	1	1	0	0

b DFS in non–triple-positive patients

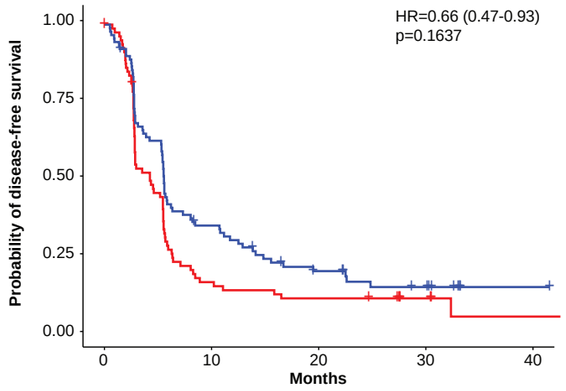

No. at risk						
Atezolizumab	89	30	14	8	1	
Observation	82	13	9	4	1	

c OS in triple-positive patients

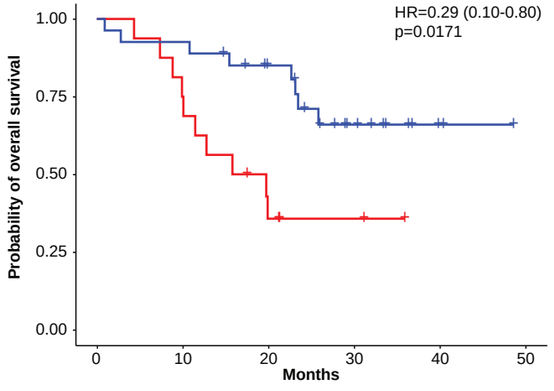

No. at risk						
Atezolizumab	27	25	19	9	2	0
Observation	16	12	5	2	0	0

d OS in non–triple-positive patients

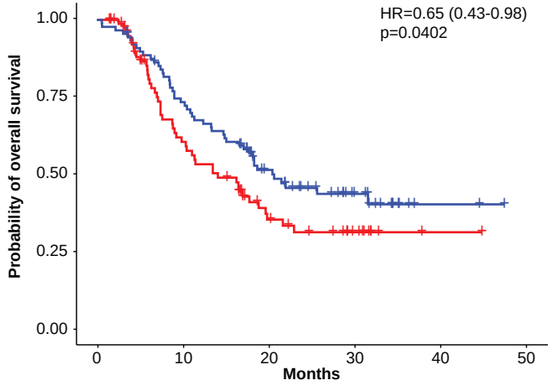

No. at risk						
Atezolizumab	89	63	36	16	2	0
Observation	82	42	19	9	1	0

Figure ED11

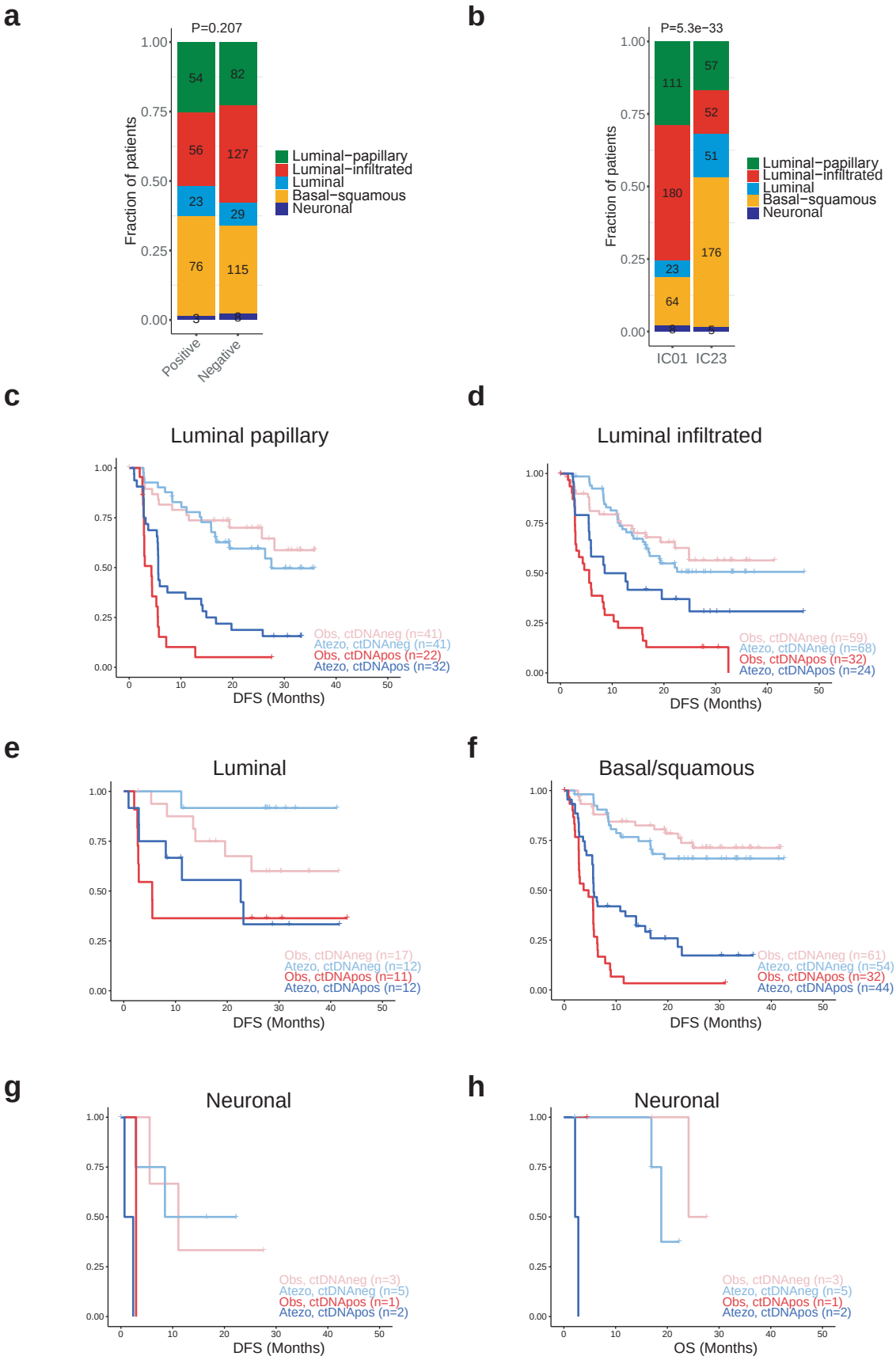
a
P=0.207
Fraction of patients
1.00
0.75
0.50
0.25
0.00
54
56
23
76
3
82
127
29
115
8
Positive
Negative
Luminal−papillary
Luminal−infiltrated
Luminal
Basal−squamous
Neuronal
b
P=5.3e−33
111
180
23
64
8
57
52
51
176
5
IC01
IC23
c
Luminal papillary
Obs, ctDNAneg (n=41)
Atezo, ctDNAneg (n=41)
Obs, ctDNApos (n=22)
Atezo, ctDNApos (n=32)
DFS (Months)
d
Luminal infiltrated
Obs, ctDNAneg (n=59)
Atezo, ctDNAneg (n=68)
Obs, ctDNApos (n=32)
Atezo, ctDNApos (n=24)
DFS (Months)
e
Luminal
Obs, ctDNAneg (n=17)
Atezo, ctDNAneg (n=12)
Obs, ctDNApos (n=11)
Atezo, ctDNApos (n=12)
DFS (Months)
f
Basal/squamous
Obs, ctDNAneg (n=61)
Atezo, ctDNAneg (n=54)
Obs, ctDNApos (n=32)
Atezo, ctDNApos (n=44)
DFS (Months)
g
Neuronal
Obs, ctDNAneg (n=3)
Atezo, ctDNAneg (n=5)
Obs, ctDNApos (n=1)
Atezo, ctDNApos (n=2)
DFS (Months)
h
Neuronal
Obs, ctDNAneg (n=3)
Atezo, ctDNAneg (n=5)
Obs, ctDNApos (n=1)
Atezo, ctDNApos (n=2)
OS (Months)